Second Wind

Final Design

Dec. 8, 2009

Josh Dowler

Caleb Meeks

John Snyder

Table of Contents

Requirements Specification.....3

Final Design.....5

Block Diagram.....6

Organization and Management.....7

Generator Motor Selection.....8

Sprockets and Chains.....9

Motor and Gearing Calculations.....11

Freewheel and Return Mechanisms.....12

Generation Stress Concentration Points.....14

Generation System Diagrams.....15

Charge Controller Design 20

Microprocessor Design.....25

Software Design.....27

Motor Controller Design.....30

Electrical Components.....31

Electronically Assisted Design.....33

Kite Retraction System Design.....43

Budget Analysis.....45

Updated Budget.....46

Schedule Analysis.....47

Gantt Chart – Fall 2009.....48

Gantt Chart – Spring 2010.....49

Appendices.....50

MAX15046 DC-DC Converter.....A

PIC18F4550 Microprocessor.....B

TLE5205-2 Motor Controller.....C

Kite Wind Generator

Requirements Specification

Overview:

Our team will design and prototype a kite wind generator. The generator will produce electrical power from the drag force applied to the kite by wind. The kite will be autonomously guided by a microprocessor to perform the gliding maneuvers necessary to produce power. A kite wind generator would be useful for generating power on large scale agricultural farms, in remote locations for disaster relief or military, or as a part of a larger wind farm.

Problem Statement:

Due to pollution and depletion of traditional energy sources there is a need to generate power from renewable energy sources. Wind is the second most abundant energy resource, next to solar energy, that can be harnessed to generate power. Kite wind generation is more effective than conventional turbines in gathering the energy from the wind for two reasons. First, the kite can reach much higher altitudes than turbines, where the wind is more reliable and strong. Second, kites can cover more area in the sky and therefore use more of the energy than a stationary turbine can. This technology could allow individuals to become energy self-sufficient and it could also be used in large scale projects as wind farms that produce high power.

Operational Description:

The kite wind generation unit will produce power based on the drag force produced by the kite in flight and the amount of line pulled, which will be connected to a generator, over time. When the kite has reached its maximum height the kite orientation will be changed to reduce its drag coefficient, and the kite will be retracted using much less power than is generated from the pull up. The kite will run autonomously in winds of 10 to 45 kilometers per hour. When the wind speeds are too high the kite will be retracted to prevent damage to the system. If the wind speeds are too low the kite will be retracted. The system will also have a user interface that displays the length of line released, and power generation. The user will also have options for three different modes of operation for the kite; deploy, sustain, and retract.

Technical Requirements:

- System will initially supply its own power to initiate energy generation and then store excess generated power
- If power generation is not sufficient to generate excess power the kite will be retracted and the user interface will run off of stored power
- System will generate at least 500 watt hours DC within 10 hours
- Kite system will be able to generate power in winds from 10 - 45 kilometers per hour
- Setup, including kite deployment, should take no more than 30 minutes
- Power generation should occur within five minutes of kite deployment
- System must have deploy, sustain, and retract modes of operation
- Autonomous control of each mode (deploy, sustain, retract)
- User interface to enable user to specify modes of operation (deploy, sustain, retract) and show user length of line released within one meter and power generated within 20 watts
- Must be able to sense length of line released within one meter and power generation within 20 watts

- System will be able to fit through a standard door frame, with width of one meter and height of two meters

Design Deliverables:

- User manual
- Drawings and schematics with analyses
- Kite generator unit
- User interface
- Parts list with associated costs
- Test report
- Final technical report

System Test Plan

1. Kite stays aloft in winds of 10 - 45 kilometers per hour
2. 10 minutes of autonomous flight and power generation in winds of 10 - 45 kilometers per hour
3. Generation of 500 watt hours DC within 10 hours
4. The electrical system will have a fail safe mechanism that will enable in case of a power surge
5. Kite retraction of less than 10 minutes in winds of 10 - 45 kilometers per hour
6. Shows accurate value for length of line released by comparing it with a tape measure within one meter
7. Shows accurate value for power generation within 20 watts by using current and voltage measurements using a multimeter

Implementation Consideration:

Follow FAA regulations part 101, subparts A and B: no flight between sunset and sunrise, a letter of intent to fly the kite above 150 feet sent to the nearest FAA ATC facility, a 100m radius of land without obstruction around base, set in an area five miles away from an airport, land must have ground visibility greater than 3 miles, and the kite line must have streamers at 50 foot intervals above 150 feet that are visible for one mile. The leads for the generator and battery will be covered to prevent shock. Sprockets and chains are part of the design and could propose some safety issues.

Final Design

Block Diagram

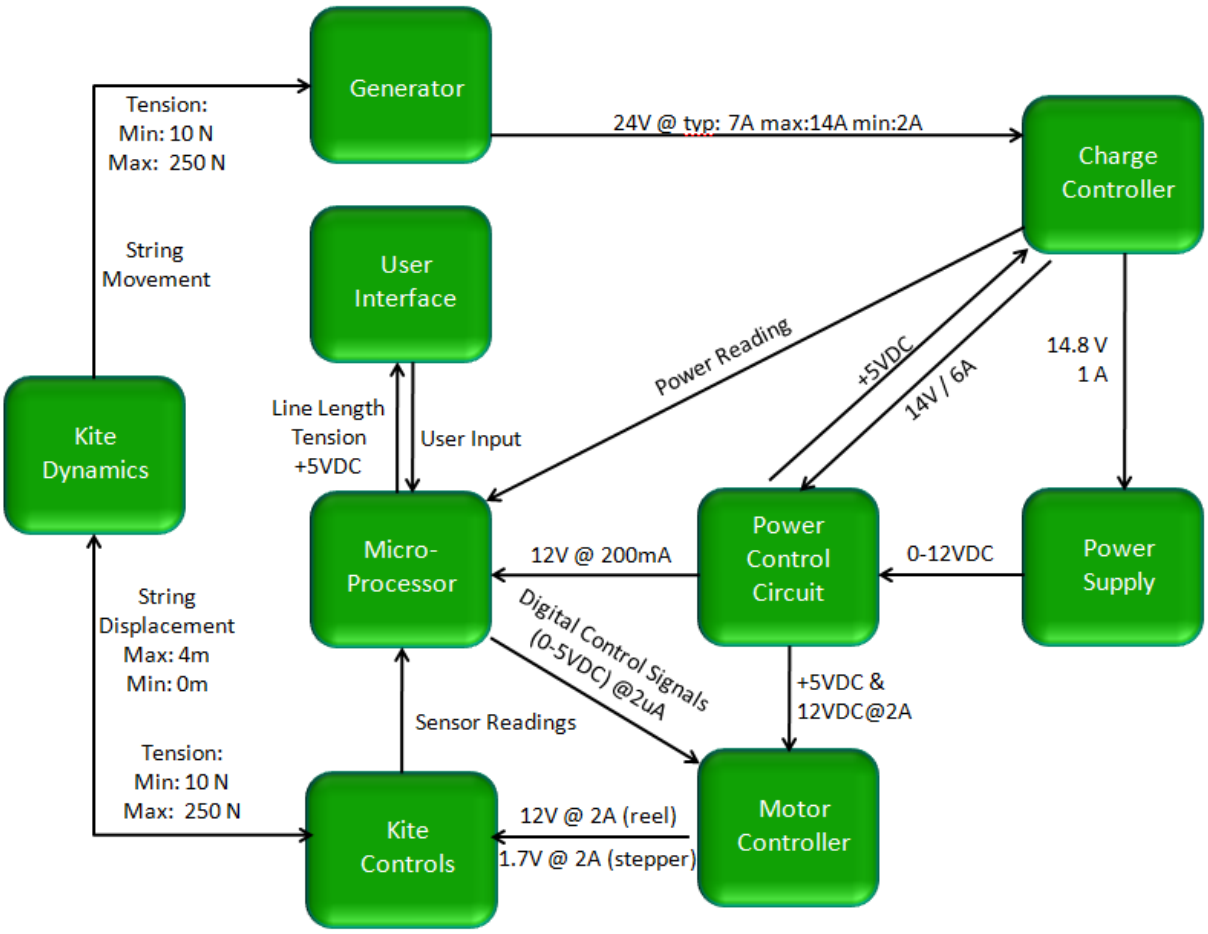

Organization and Management

John Snyder – John is a senior computer engineering student, with a 50/50 electrical and engineering and computer science split. He will be working with programming the microprocessor to get it to work with the motor controller, kite controls system, and the user interface. He will also be working on the charge controller to prevent it from overcharging and surge protection for the power supply. He will also be working with different sensors to provide information for the system.

Josh Dowler – Josh is a senior mechanical engineering student, and is the project leader. He will be in charge of converting the tension provided by the kite behavior and turning it into electric power. He will be working with the generator motor and a freewheel mechanism to allow the kite to retract without affecting the generator and selecting gear ratios as necessary. As project leader, he will be in charge of managing the budget, overseeing all project happenings, and reviewing documentation.

Caleb Meeks – Caleb is a senior mechanical engineering student. He will be in charge of working with the controls system and kite behavior. He will construct and work closely with John on the electrical and mechanical aspects of the controls system. The controls system will also link with the power generation processes, and therefore Caleb and Josh will be working to integrate their systems.

All team members will contribute equally to any documentation that will be presented, including reports and oral presentations. Each team member will be in charge of maintaining their notebooks and doing research on their respective parts outside of group meeting times. Team members are required to attend team meetings unless they notify the other team members about their absence.

Generator Motor Selection

Ideal motor criteria:

1) Reversible - motor can act as a generator
2) DC - no AC/DC inverter needed
3) Permanent Magnet - powerful
4) Brushless - less friction loss
5) Low rated RPM - less gearing required
6) Continuous Duty - made to run continuously

Motor Torque in*lbf (N*m)	Gear Ratio	Kite Tension lbf (N)	Motor Power (watts)
1.0 (0.113)	7.4	3.5 (15.6)	30.76
2.0 (0.246)	7.0	7.0 (31.1)	61.53
3.0 (0.369)	7.0	10.5 (46.7)	92.29
4.0 (0.492)	7.0	14.0 (62.3)	123.05
5.0 (0.615)	7.0	17.5 (77.8)	153.82
6.0 (0.738)	7.0	21.0 (93.4)	184.58
7.0 (0.861)	7.0	24.5 (109.0)	215.34
8.0 (0.984)	7.0	28.0 (124.6)	246.11
9.0 (1.107)	7.0	31.5 (140.1)	276.87
10.0 (1.230)	7.0	35.0 (155.7)	307.63
11.0 (1.353)	7.0	38.5 (171.3)	338.40
12.0 (1.476)	7.0	42.0 (186.8)	369.16
13.0 (1.599)	7.0	45.5 (202.4)	399.92
14.0 (1.722)	7.0	49.0 (218.0)	430.68
15.0 (1.845)	7.0	52.5 (233.5)	461.45
Assuming a 4" diameter spring return mechanism			

Table 1

Based on some basic lift and drag force equations ($L = \frac{1}{2}\rho v^2 A C_L$, $F_d = \frac{1}{2}\rho v^2 C_d A$) tension force from the kite onto the system was calculated. In these equations; *p* is air density, *v* is the wind speed, *A* is the characteristic area of the kite, and C_l and C_d are the lift and drag coefficients, respectively. The tension force was then converted into a torque value $\boldsymbol{\tau} = \mathbf{r} \times \mathbf{F}$, based on assumed values for sprockets used to gear the system. The torque transferred to the motor varied based upon the assumed values for the sprockets, so an Excel spreadsheet was used to calculate various possible torque values that could be transferred to the motor based upon the gearing ratio and the speed of the kite pulling out (Figure 2).

Based upon the calculated torque that could be supplied to the system our system will be able to overcome the torque for a 350 watt motor. Many inexpensive brushed motors are available with power outputs around 350 watts. One brushless motor was found that had a power output in the range of 350 watts. However, this motor is not reversible and thus cannot be used as a generator

The chosen motor is priced at $47.91 from Monster Scooter Parts shown in table 1. The motor has an 11 tooth sprocket for #25 roller chain. The system will need a form of gearing to reach the rated motor speed.

Model:MY1016

Voltage/V	24V/36V	24V/36V	24V/36V	24V/36V
Rated Power/W	200W	250W	300W	350W
No-load Current/A	≤1.5/1.0	≤1.6/1.2	≤1.8/1.4	≤2.0/1.4
No-load Speed/RPM	3300	3350	3400	3450
Rated Torque/N·m	0.70	0.90	1.04	1.22
Rated Speed/RPM	2700	2650	2750	2750
Rated Current/A	≤10.6/7.1	≤13.4/8.9	≤16.0/10.7	≤18.7/12.5
Eff./%	≥76	≥78	≥78	≥78
Main Application	Small electric cars, scooters			

Table 2

Sprockets and Chains

The design of the gearing system began during the generator motor selection phase due to the dependency between the two systems. The force coming in from the lines needs to be geared up to supply the rated RPMs of the motor.

The use of belts and pulleys were considered along with chains and sprockets. However, it soon became apparent that belts and pulley are much more expensive and difficult to find in varying sizes. The efficiencies of chains and belts are both above 95%, so this was not a factor. A decision matrix was used to analytically make this decision. Chains are obviously the better choice for this system.

Attribute	Weight		Chains	Belts
Cost	0.5		7	5
Efficiency	0.2		9	9
Availabilty	0.2		9	5
Durability	0.1		7	5
Total	1		7.8	5.8

Table 3

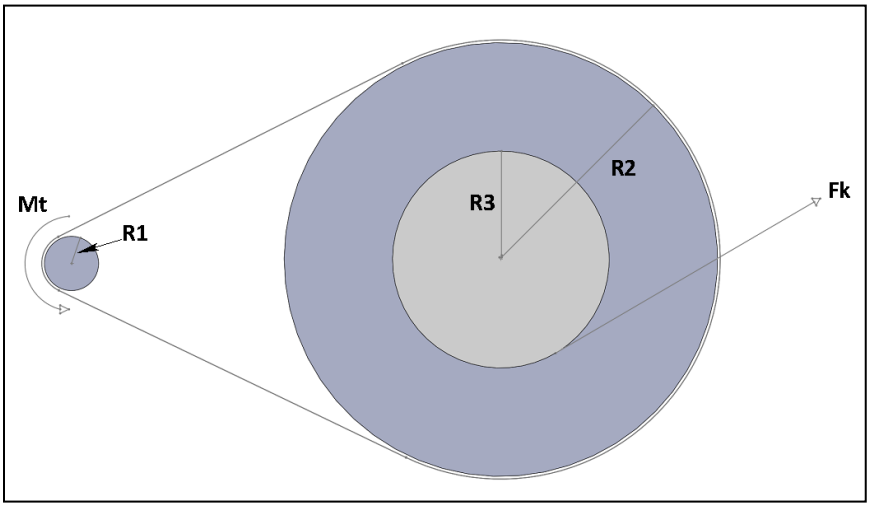

Figure 1

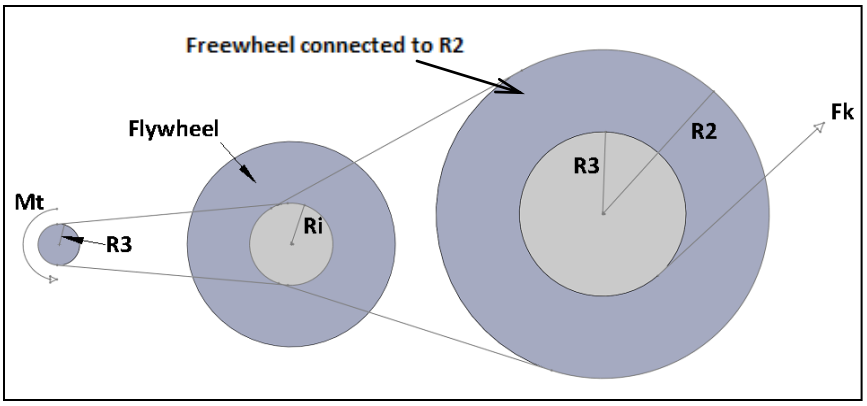

Figure 2

The initial design used only one shaft on which a large gear would sit with the return mechanism and directly connect to the motor (Figure 1). However, it was soon determined that the addition of an intermediate shaft was necessary to allow for proper use of the freewheel mechanism when connected to the large sprocket (Figure 2). The intermediate shaft, which contains two sprockets and a flywheel, connects the drive shaft and the motor sprocket. This means that the first shaft contains the spring return mechanism and the large sprocket connected to the freewheel system. This configuration, in conjunction with the flywheel, allows the intermediate shaft, and therefore the motor, to continue spinning between the oscillatory pull of the kite on the system.

The generator motor uses #25 roller chain, therefore the sprockets must also use #25 roller chain. The tension of the kite lines at maximum wind speed is 50.97 lbs (226.75 N), as calculated from the lift and drag force equations stated earlier. The working load of #25 roller chain is 140 lbs (622.75 N) which gives a factor of safety of 2.75 for the chains. The designed system gearing ratio will be 7.4:1, which will give a balance between the kite speed required and the torque the kite tension force will generate. The Excel data and graph is shown on the following page in Figure 3 and Table 4.

A fully assembled rear wheel assembly comes with the large sprocket combined with the freewheel, and axle size needed as well as a wheel and tire that is not needed. Two sprockets (one 14 tooth and one 16 tooth), a steel bar of ½ inch diameter, and two bearings for the intermediate shaft will be purchased.

The flywheel does not have a specific design as of yet. From research it has been found that the heavier the flywheel the smoother the operation of the motor, as long as the driving force is able to overcome the inertia of the flywheel. The design portion on flywheels in the machine design text book is not clear in the actual process for designing the flywheels. There are also no online resources that use an engineering approach to designing flywheels.

I will continue to do more research on the design of flywheels.

Motor and Gearing Calculations

Mt (in*lbs)	R1 (inch)	R2 (inch)	R3 (inch)	Fk (lbs)		Mr (RPM)	Ks (in/min)	Ks (ft/sec)
11	0.5	1.5	2	16.5		2750	11519.17	16.00
11	0.5	1.6	2	17.6		2750	10799.22	15.00
11	0.5	1.7	2	18.7		2750	10163.98	14.12
11	0.5	1.8	2	19.8		2750	9599.31	13.33
11	0.5	1.9	2	20.9		2750	9094.08	12.63
11	0.5	2	2	22		2750	8639.38	12.00
11	0.5	2.1	2	23.1		2750	8227.98	11.43
11	0.5	2.2	2	24.2		2750	7853.98	10.91
11	0.5	2.3	2	25.3		2750	7512.50	10.43
11	0.5	2.4	2	26.4		2750	7199.48	10.00
11	0.5	2.5	2	27.5		2750	6911.50	9.60
11	0.5	2.6	2	28.6		2750	6645.68	9.23
11	0.5	2.7	2	29.7		2750	6399.54	8.89
11	0.5	2.8	2	30.8		2750	6170.99	8.57
11	0.5	2.9	2	31.9		2750	5958.19	8.28
11	0.5	3	2	33		2750	5759.59	8.00
11	0.5	3.1	2	34.1		2750	5573.79	7.74
11	0.5	3.2	2	35.2		2750	5399.61	7.50
11	0.5	3.3	2	36.3		2750	5235.99	7.27
11	0.5	3.4	2	37.4		2750	5081.99	7.06
11	0.5	3.5	2	38.5		2750	4936.79	6.86
11	0.5	3.6	2	39.6		2750	4799.66	6.67
11	0.5	3.7	2	40.7		2750	4669.94	6.49
11	0.5	3.8	2	41.8		2750	4547.04	6.32
11	0.5	3.9	2	42.9		2750	4430.45	6.15
11	0.5	4	2	44		2750	4319.69	6.00
11	0.5	4.1	2	45.1		2750	4214.33	5.85
11	0.5	4.2	2	46.2		2750	4113.99	5.71
11	0.5	4.3	2	47.3		2750	4018.32	5.58
11	0.5	4.4	2	48.4		2750	3926.99	5.45
11	0.5	4.5	2	49.5		2750	3839.72	5.33
11	0.5	4.6	2	50.6		2750	3756.25	5.22
11	0.5	4.7	2	51.7		2750	3676.33	5.11
11	0.5	4.8	2	52.8		2750	3599.74	5.00

Table 4

The variables in Table 4 are defined in Figure 1 on page 12. R2 is varied to find the radius of the large sprocket needed to attain a balance between kite speed (Ks) and force of the kite (Fk).

A gear ratio that balances kite speed and force of the kite can be determined using the graph of Figure 3. This gives a gear ratio R2:R1 of approximately 7.4:1. Thus the kite will need to move around 6.5 feet per oscillation of the system based on Table 4.

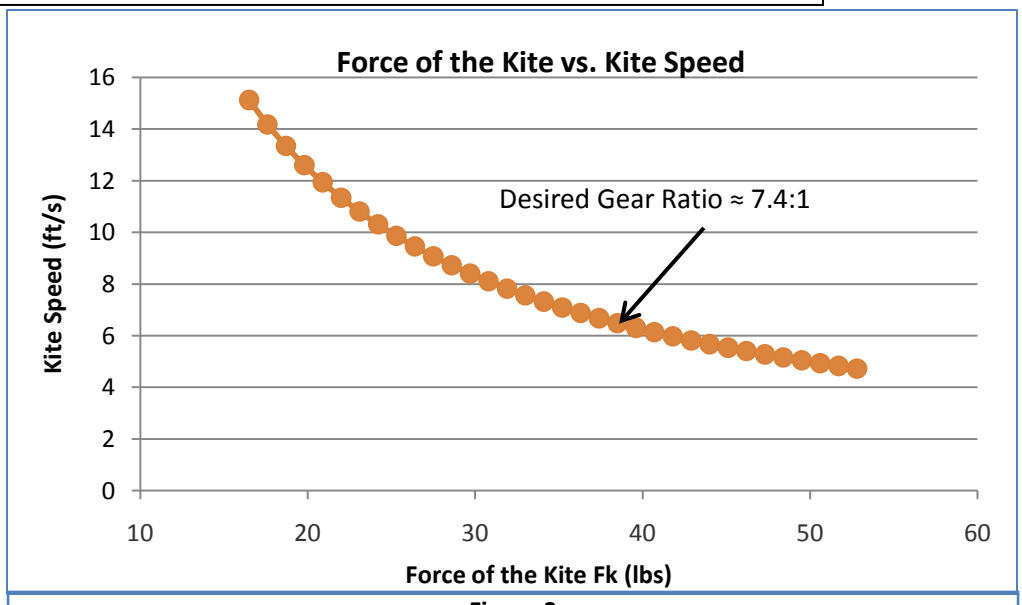

Figure 3

Freewheel and Return Mechanism

The freewheel mechanism is a vital part of the generation system design. Figure 4 shows how a basic freewheel mechanism works. A freewheel allows free rotation in one direction, but when spun in the opposite direction the system engages and allows energy transfer. This means that the kite string, when pulled out, will engage the freewheel and transfer energy into the shafts and motor. However, when the kite is in the return stage of its oscillatory motion, due to the spring return mechanism, the kite string and the motor can move independently.

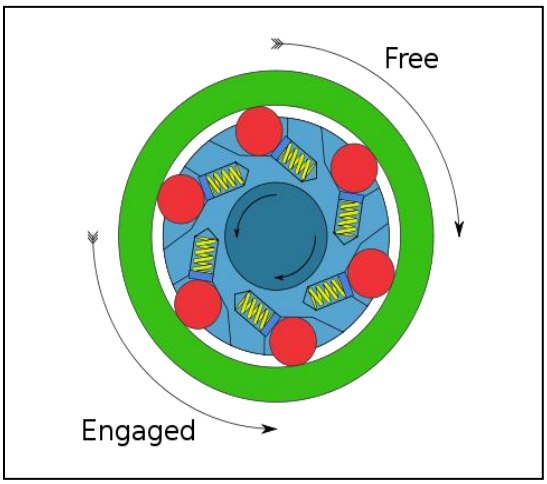

Figure 4

This system will use a freewheel that is already attached to a sprocket and axle on a rear wheel assembly of an electric scooter. There are no force or life specifications on the freewheel that we will be using. However, it is assumed that this system will undergo far less stress compared to a high powered electric scooter that the part is made for.

The return mechanism is the system that will be used to retract the kite during each oscillation of the kite through its figure eight pattern. The return mechanism consists of a spring that will store some of the energy of the kite into potential spring energy when the kite is on its outward pull. The potential spring energy will then be released when the kite is on the outside of its figure eight flight pattern, which will be discussed later, and the kite will be retracted to its original position.

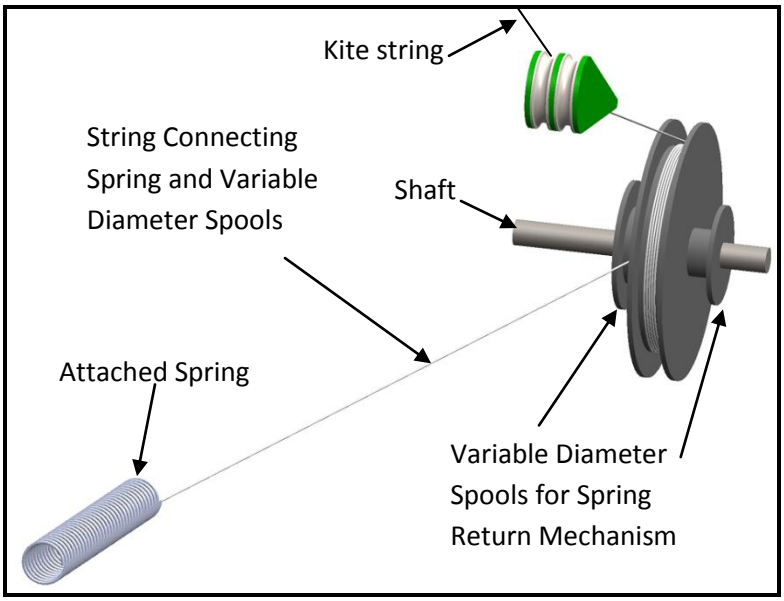

Figure 5

The spring return mechanism is more difficult to design due to the need for a constant kite pull out length at varying wind speeds. R3 (Figure 2) needs to remain constant at 2 inches due to the gearing ratio already being selected. The values for the force of the kite are already known as shown in Table 5. The cheapest and easiest way to allow the kite to have a constant pull out length at varying wind speeds is to vary the spring constant 'k' of the spring. Under the budget of this

project the best way to do that is to have the operator manually adjust the spring for the current relative wind speed. Setting the torque of the kite on the shaft equal to the torque a spring on the shaft allowed iteration to find a 'k' and spring extension 'ΔX' that could be manufactured and purchased.

The springs found for minimum and average winds happened to be able to use the same radius 'R0' that is defined in Figure 5 as the variable diameter spools for spring return mechanism. The spring found for the maximum wind speed required a smaller R0 to allow for the necessary six feet as seen on the motor and gearing calculations page. The use of a linear spring was determined by the wide variety of linear springs over torsion springs on the market. Furthermore, linear springs generally have a smaller 'k' value which will allow the kite to meet its displacement requirements during oscillation.

The springs being used by this system are from W.B. Jones Spring Company Inc. W.B. Jones offers quick and easy purchase of a number of stock linear springs. Table 6 shows the specifications for the three springs chosen for minimum, average, and maximum wind speed values.

F_{min} (lbf)	R3 (in)	=	k (lbf/in)	ΔX (in)	R0 (in)
3.48	2.00	=	2.95	9.42	0.25
3.48	2.00	=	1.31	14.14	0.38
3.48	2.00	=	0.74	18.85	0.50
3.48	2.00	=	0.47	23.56	0.63
3.48	2.00	=	0.33	28.27	0.75
3.48	2.00	=	0.24	32.99	0.88
3.48	2.00	=	0.18	37.70	1.00
3.48	2.00	=	0.15	42.41	1.13
3.48	2.00	=	0.12	47.12	1.25
3.48	2.00	=	0.10	51.84	1.38
F_{avg} (lbf)	R3 (in)	=	k (lbf/in)	ΔX (in)	R0 (in)
15.87	2.00	=	13.47	9.42	0.25
15.87	2.00	=	5.99	14.14	0.38
15.87	2.00	=	3.37	18.85	0.50
15.87	2.00	=	2.16	23.56	0.63
15.87	2.00	=	1.50	28.27	0.75
15.87	2.00	=	1.10	32.99	0.88
15.87	2.00	=	0.84	37.70	1.00
15.87	2.00	=	0.67	42.41	1.13
15.87	2.00	=	0.54	47.12	1.25
15.87	2.00	=	0.45	51.84	1.38
F_{max} (lbf)	R3 (in)	=	k (lbf/in)	ΔX (in)	R0 (in)
50.58	2.00	=	42.93	9.42	0.25
50.58	2.00	=	25.80	12.16	0.32
50.58	2.00	=	17.20	14.89	0.40
50.58	2.00	=	12.28	17.62	0.47
50.58	2.00	=	9.20	20.36	0.54
50.58	2.00	=	7.15	23.09	0.61
50.58	2.00	=	5.72	25.82	0.69
50.58	2.00	=	4.68	28.56	0.76
50.58	2.00	=	3.90	31.29	0.83
50.58	2.00	=	3.29	34.02	0.90

Table 5

	Outer Dia. (in.)	Wire Dia. (in.)	Free Length (in.)	Part No.	Rate (lbs / in)	Load (lbs)
Fmin	0.875	0.062	8.500	137	0.34	6.17
Favg	0.500	0.072	20.000	774	1.55	16.89
Fmax	1.250	0.162	12.000	346	12.50	62.45

Table 6

Generation System Finite Element Analysis

Finite Element Analysis was completed on the shaft that would have the most likelihood to fail. This is due to the large load of the flywheel on the shaft as well as the two intermediate sprockets. There is a force of 50 lbs (N) in the center of the shaft, where there would actually be a weight of 25 lbs (N). There are also two torsion forces where the intermediate sprockets will go with a value of 22 lb*in (), where there would actually be only as much as 11 lb*in of torque.

Figures 6, 7, and 8 below represent the deflection, stress, and factor of safety of the beam with exaggerated deflections. The deflections are well below one thousandth of an inch. This proves that the shaft will easily support the forces acting on it.

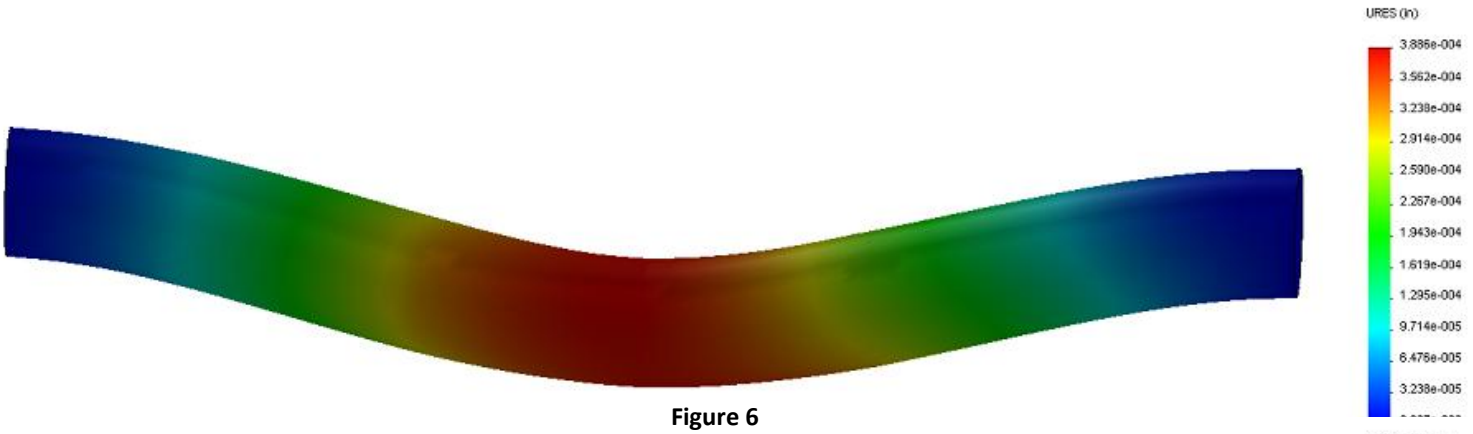

Figure 6

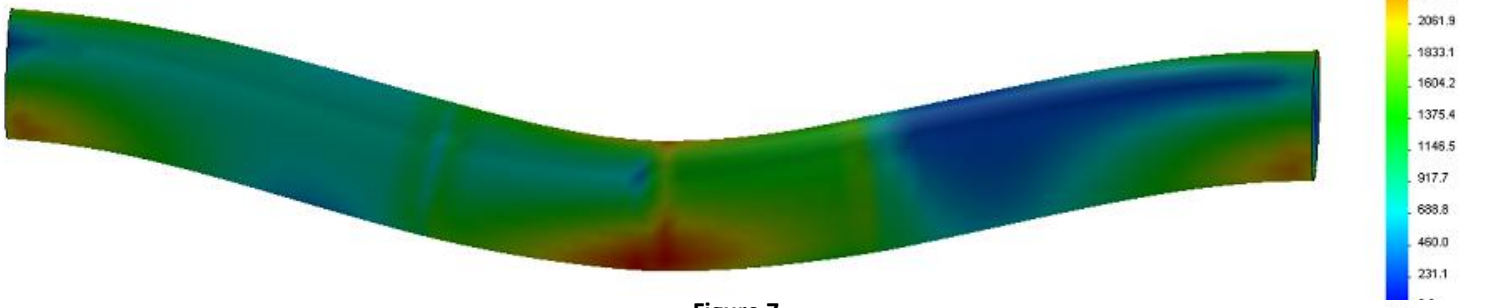

Figure 7

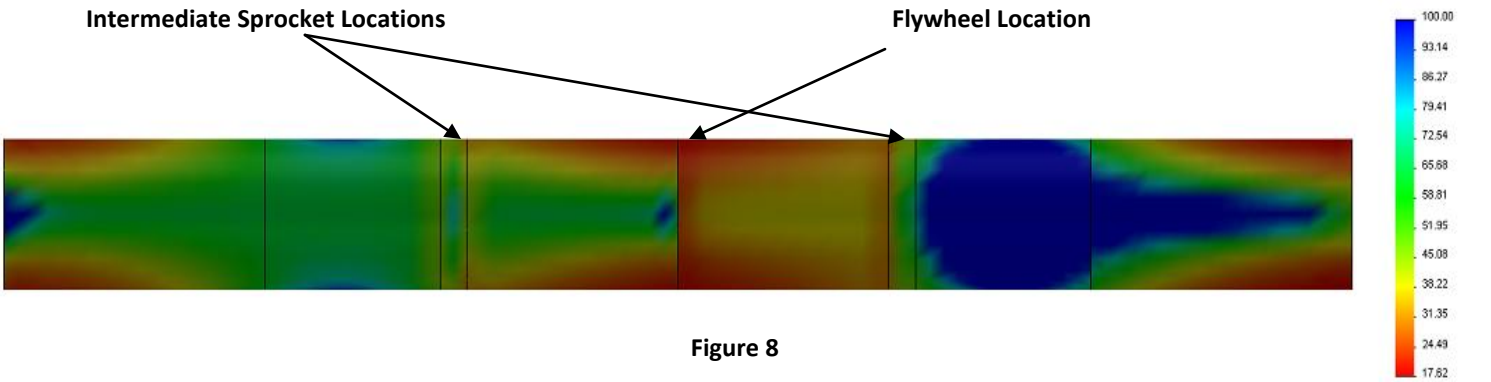

Figure 8

Power Generation System Diagram

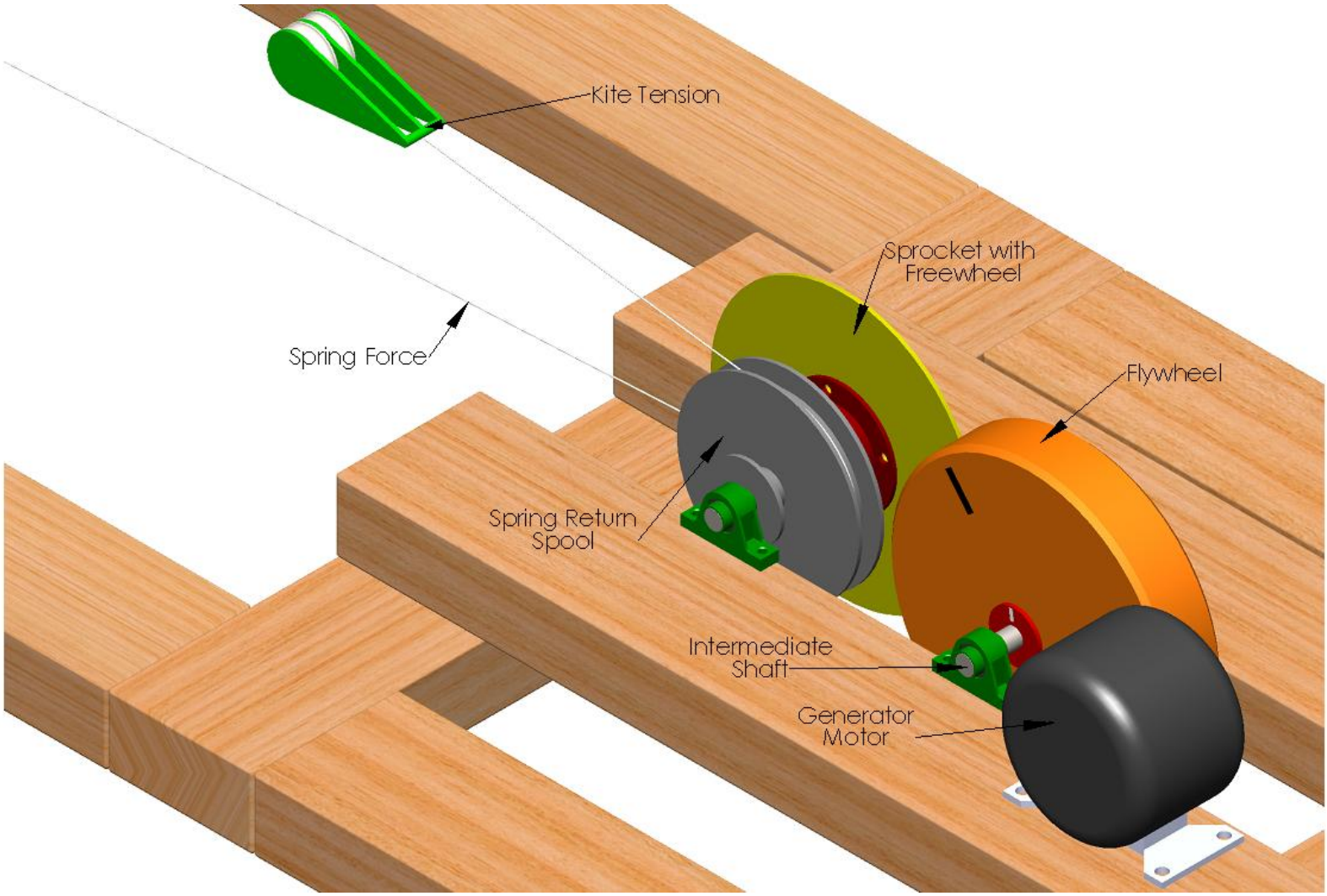

Power Generation System Diagram (Cont.)

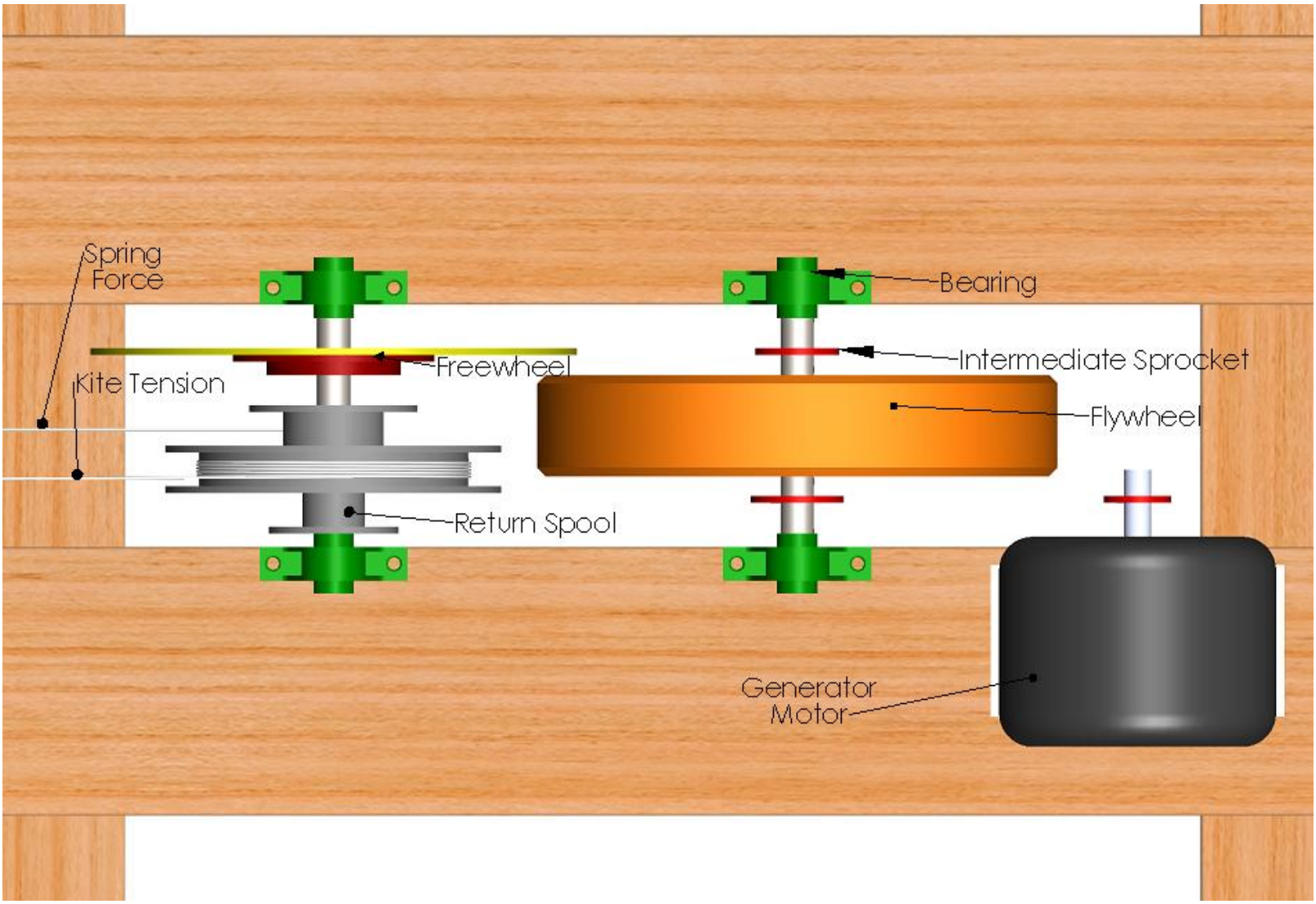

Power Generation System Diagram (Cont.)

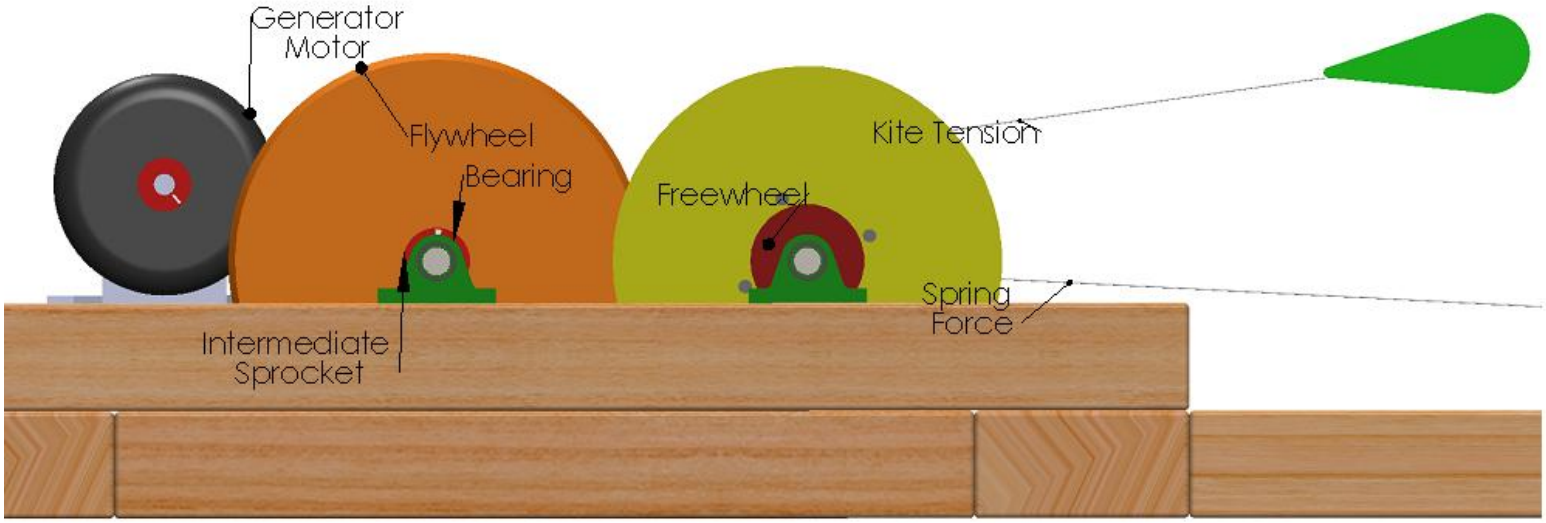

Power Generation System Diagram (Cont.)

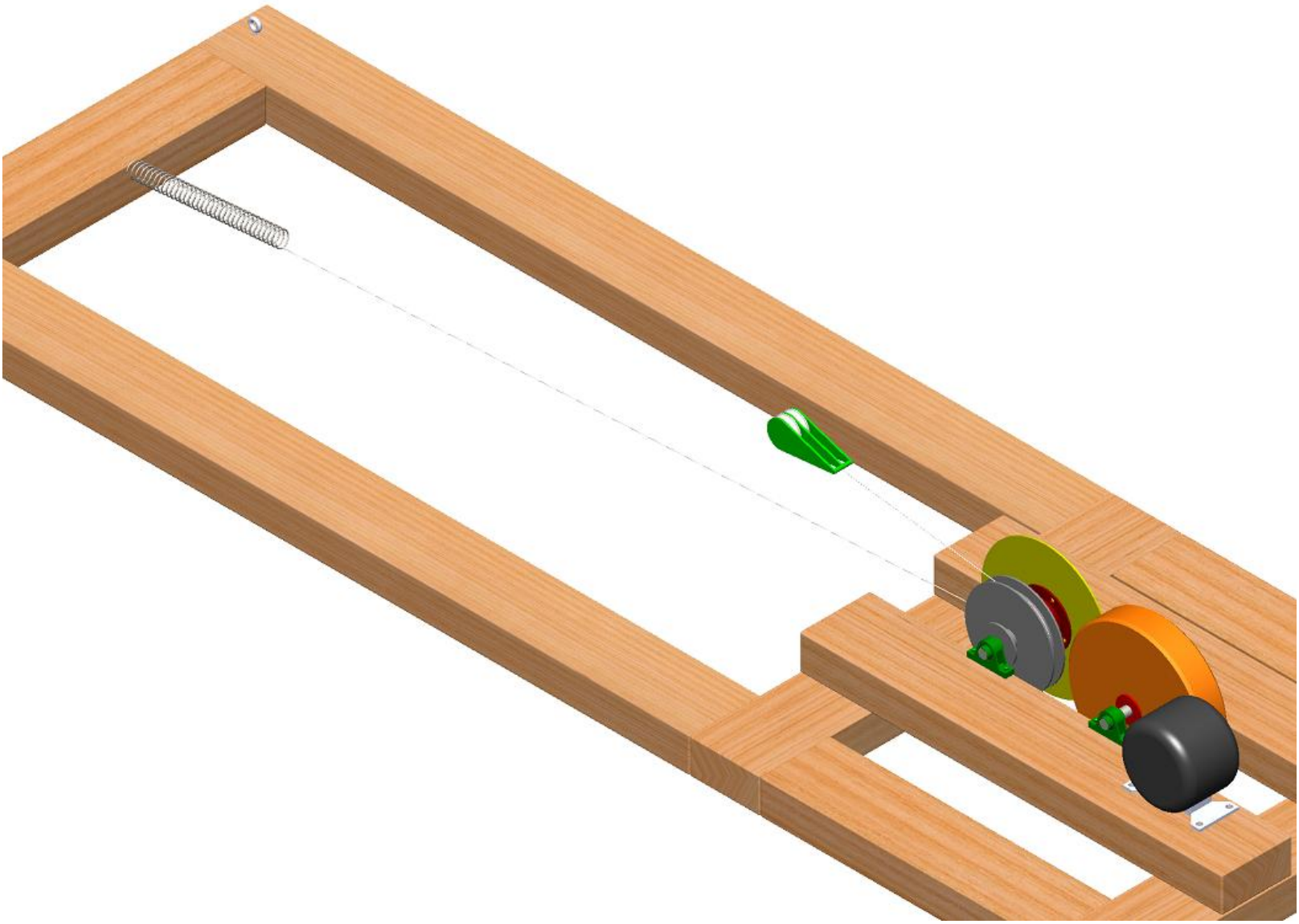

Power Generation System Diagram (Cont.)

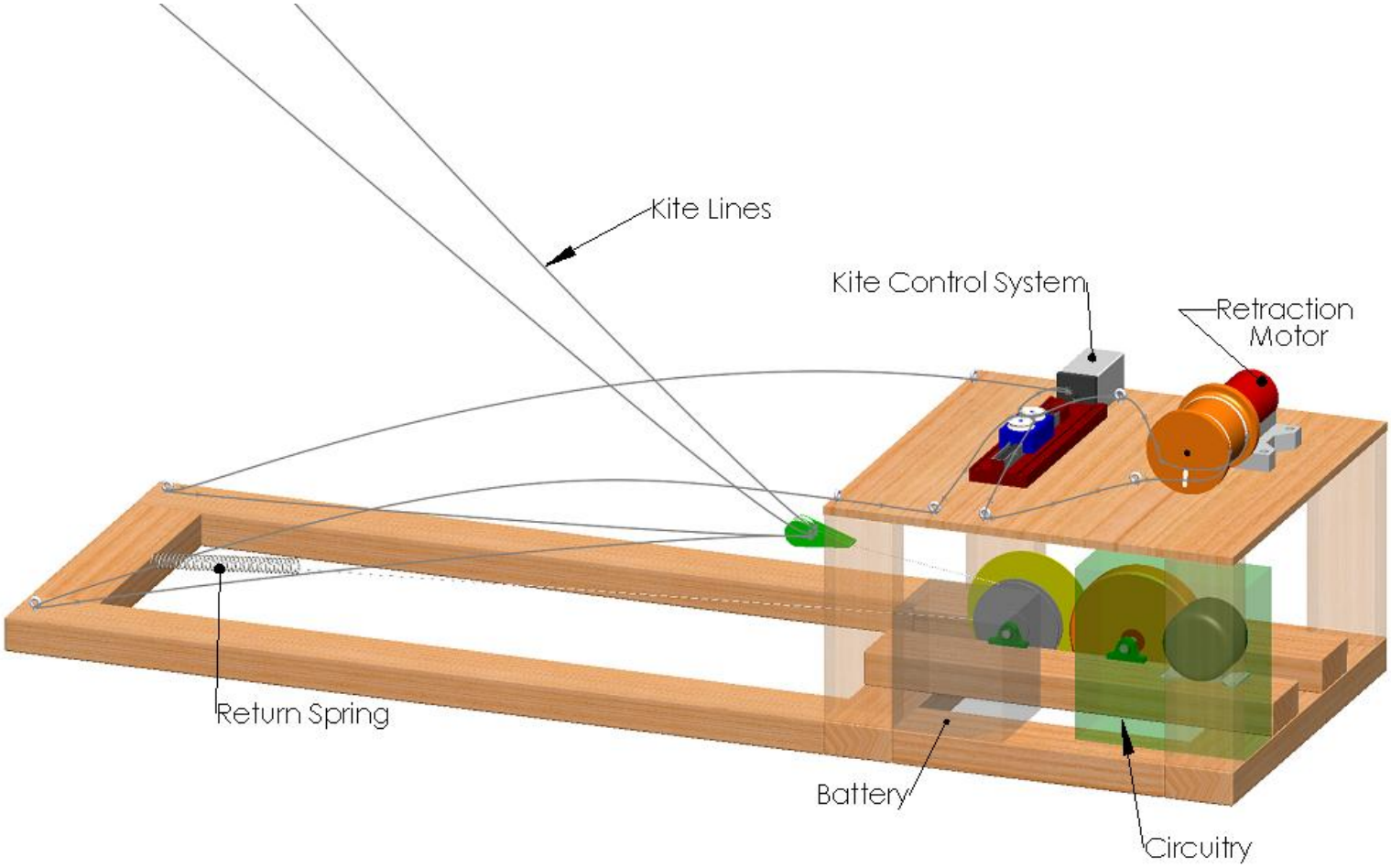

Charge Controller Design

Development of a proper charge controller for our application required the consideration of many different factors. This begins with the motor that is generating our power. We have a 24V, 350W DC motor as our generator. This means the charge controller needs to be able to handle high voltage (up to 24V) and high current inputs (up to 14A). It then needs to regulate those high inputs into a manageable power source to charge a battery. The battery chosen is a 12V 26Ah lead acid battery. This battery will allow a capacity of 312 watt hours. The entire system needs to prove it can generate 500 watt hours within a ten hour period. Since storing all of this energy to the battery is not possible, the current and voltage generated will be monitored over that time to compute the average energy production.

Since constant current and voltage generation measurements need to be taken to output the instantaneous power generation to an LCD screen, sensors that were rated to handle a high power input needed to be acquired. Some possible sensors looked into were current monitor ICs using high side current shunt and a simple Hall Effect current sensor (uses the electrical fields produced by the current to produce potential). Most current monitor ICs are rated for very low currents therefore they were irrelevant to the application of the project. The Hall Effect sensors seemed promising, but it would have been a lot of extra design work to create the current sensor circuit which would be outside our time constraints. Both the current and voltage ICs were found from a company called Phidgets which provides prebuilt circuits rated high enough to handle our power and still stay within our budget.

Once a way to monitor power was discovered, the next roadblock was voltage and current regulation. The Maxim MAX15046 is a 40V, high-performance, synchronous Buck controller. This chip (while it is complex) provided the exact regulation needed all for less than five dollars per IC. This IC accepts an input voltage from 4.5V to 40V and outputs a fixed voltage that can be configured between the range of .6V to 85% of V_{in}. It also provides up to a 25A output capability. This will allow stable voltage to be provided to the battery. In parallel with the battery there is a Zener diode to act as overcharge protection. After the battery, the sources run into other regulators that will provide ample voltage to the motors, microprocessor, and other IC chips.

Current Monitor Decision

Criteria	Weights	Phidgets 30A Current Monitor	Allegro ACS712	TI INA219	Hall Effect Current Monitor
Effectiveness	0.4	9	8	3	7
Practicality	0.2	9	5	3	5
Time	0.25	7	2	1	1
Cost	0.15	5	9	7	8
TOTALS	1	7.9	6.05	3.1	5.25

Table 8 - current monitor mechanism decision matrix

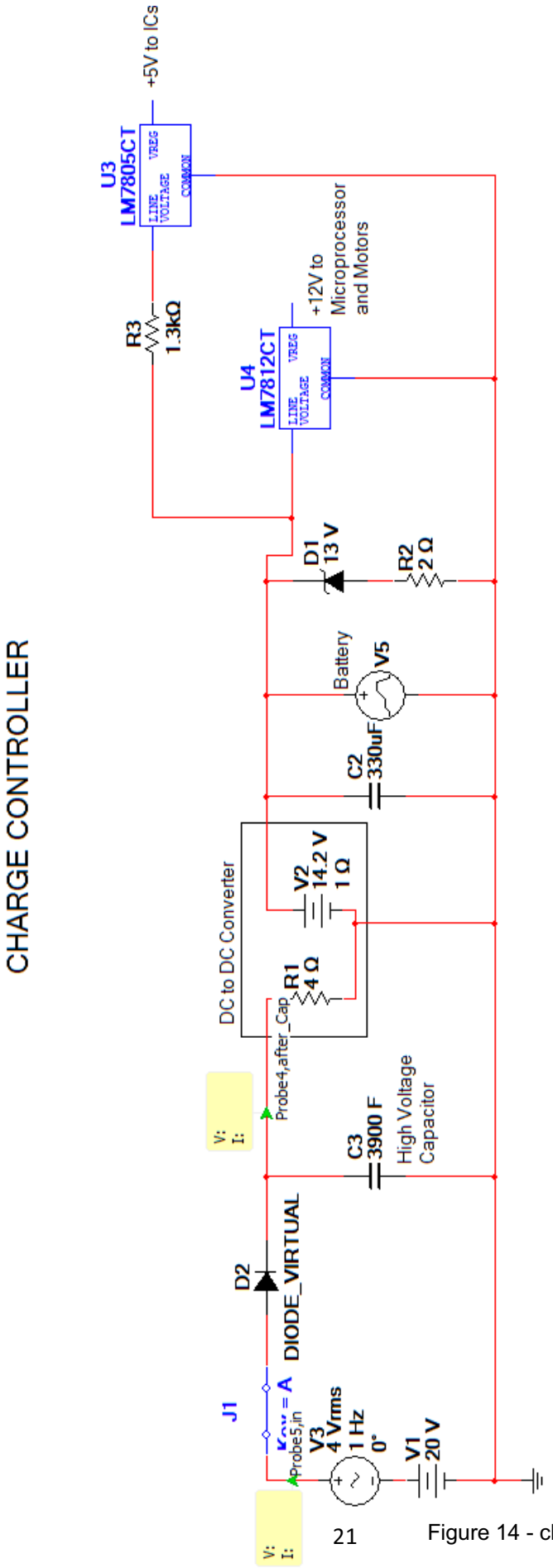

Figure 14 - charge controller circuit diagram

DC-DC Converter

As afore stated, the Maxim MAX15046 is a 40V, high-performance, synchronous Buck controller is the switching regulator chosen as a part of the charge controller design. This chip (while it is complex) provided the exact regulation needed all for less than five dollars per IC. This IC accepts an input voltage from 4.5V to 40V and outputs a fixed voltage that can be configured between the range of .6V to 85% of V_{in}. It also provides up to a 25A output capability. This will allow stable voltage to be provided to the battery.

The MAX15046 is excellent for the specifications it needs to meet for the project however it requires a lot of external circuitry and can't be modeled easily is MultiSim. The MAX15046 is a pulse width modulated controller which uses a frequency to step down the voltage from the input. Despite not being able to be easily simulated, the MAX15046 comes with exact specifications how to calculate the values of the external components. Beginning on Appendix A7, the equations for the external components can be found. These equations are given to find the effective input-voltage range, set the output voltage, set the switching frequency, determine the inductor used, set the valley current limit, and determine the input and output capacitors.

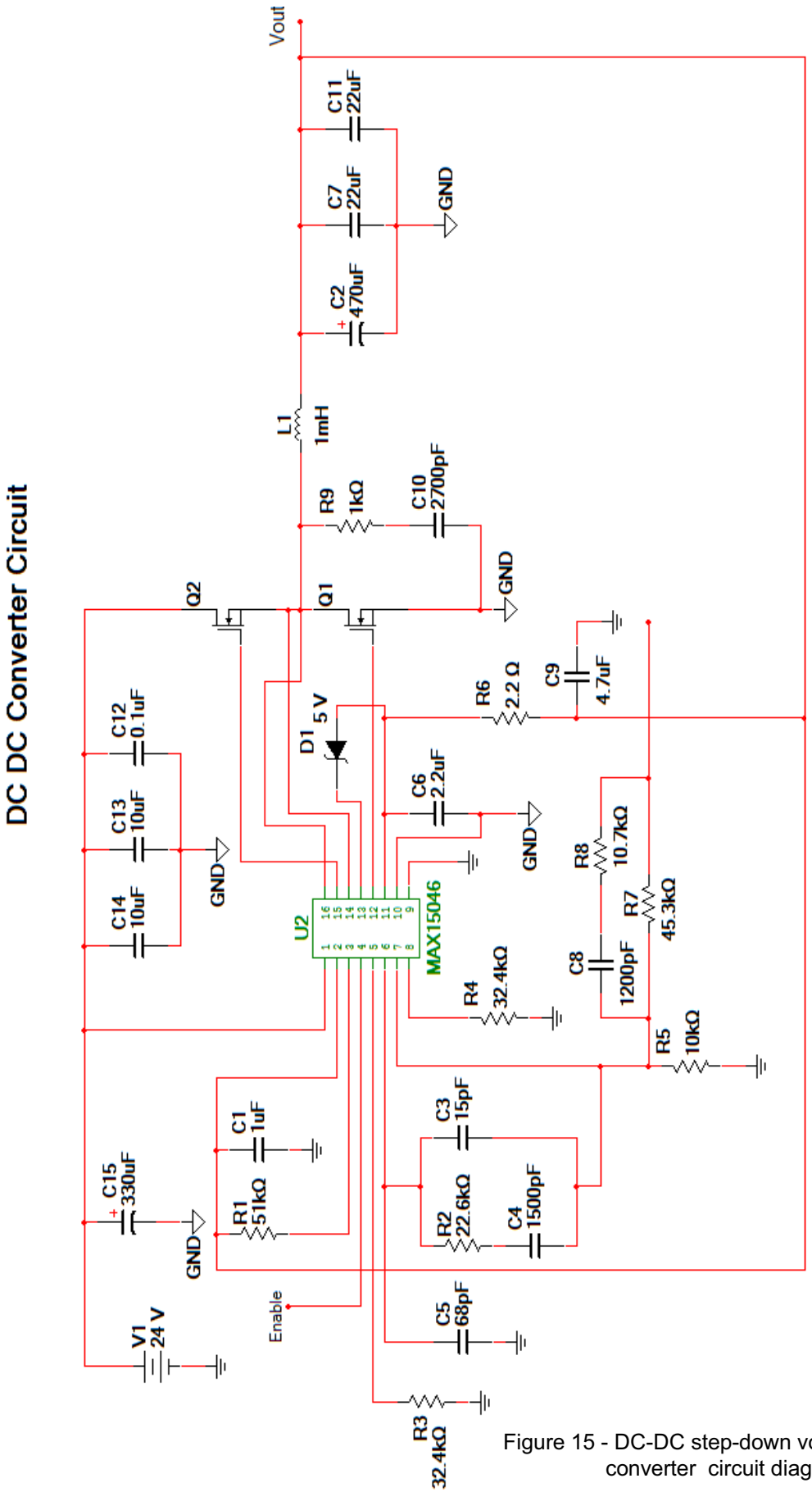

Figure 15 - DC-DC step-down voltage converter circuit diagram

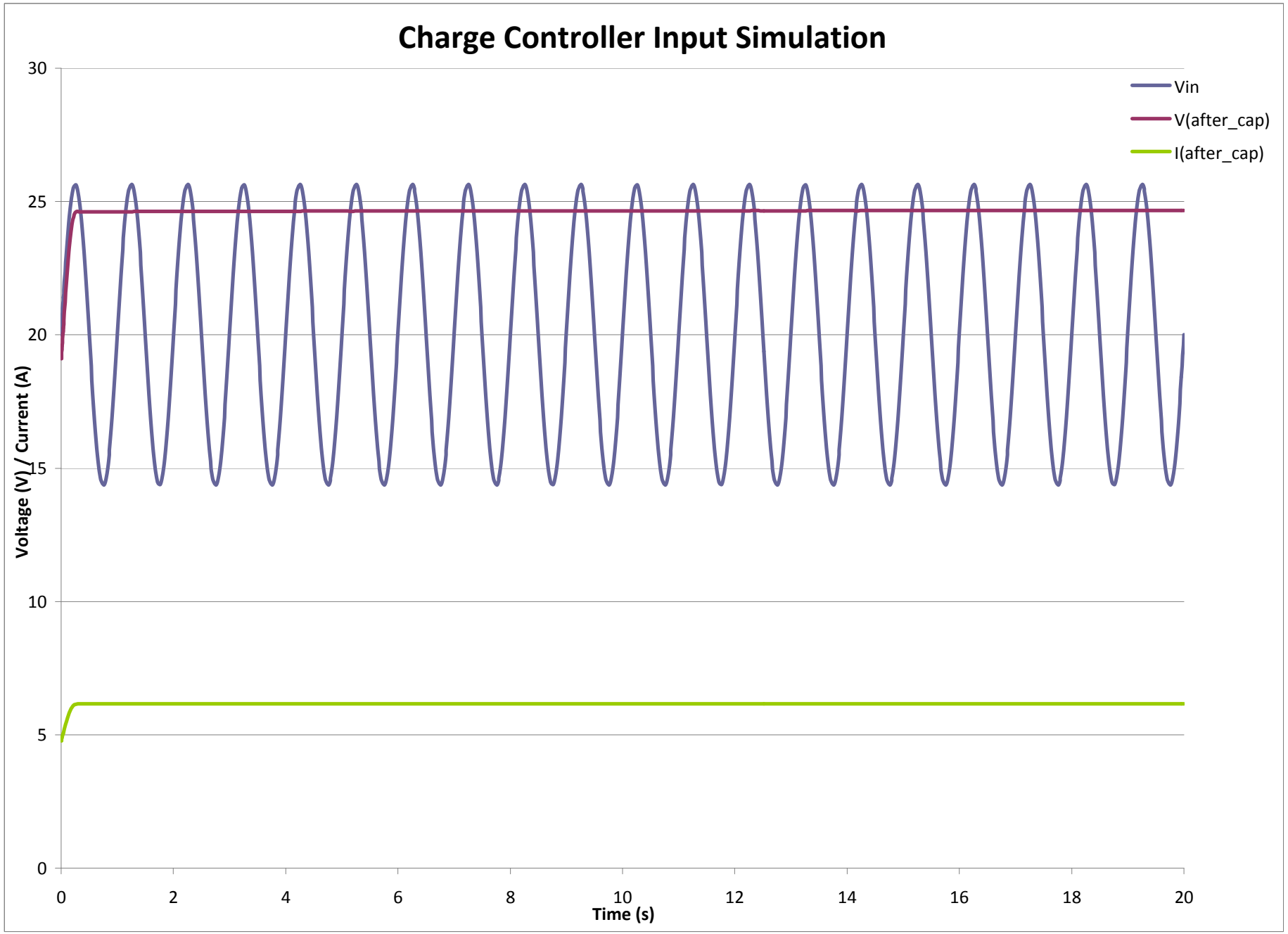
Charge Controller Input Simulation
Vin
V(after_cap)
I(after_cap)
Voltage (V) / Current (A)
Time (s)
0
5
10
15
20
25
30
0
2
4
6
8
10
12
14
16
18
20

Microprocessor Design

The microprocessor needs to be chosen based upon what inputs and outputs it needs to have for the current project. After the kite system conceptualization, ideas of what is needed in a microprocessor are formed. The need to monitor the current and voltage to calculate the power is first understood. There is also need for an input to measure the length of string released as well as a need for four inputs to measure the kite string angles to determine the kite's relative position in the air. Finally, a tension sensor input is necessary to be able to scale calculations up or down depending on wind speed. All of these inputs require at least 8 A/D Inputs. A/D inputs will also be needed for the three way user mode switch on the user interface. This switch allows the user to let the kite ascend, retract, or sustain. The other portion of the user interface is the LCD screen which will output the length of line released and the instantaneous power generation measured. The LCD screen will require five I/O ports on the microprocessor. The last feature the microprocessor needs is a pulse width modulation system to control the two motors.

Another important consideration taken with the microprocessor is time. Development time is a significant factor in building the electrical system. This led to the need for a development board. A development board allows the programmer to easily write software for the microprocessor and upload it without having the hassle of a using a microchip programmer and designing a PCB board for the microprocessor. The only downfall is the expense that arises with development boards. If a single microprocessor was purchased it would cost $4-6. The development board cost close to $50. This cost was worth the time that would have been lost if a standalone microprocessor was purchased. To view the trade-off decision matrix for microprocessor selection, see table 8.

All of these considerations led to the Microchip PIC18F4550 Development Board from Futerlec.com. This is a development board within budget that meets all the criteria needed for inputs and outputs, and it even allocates some extra features.

All of the sensors will have to be checked on a constant basis and be locked in a continuous loop to keep the kite in flight. The only exceptions will be user-mode changes from the user interface. This switch will trigger interrupts in the microprocessor and alter the flow of the program which will resume once the interrupt is completed. In figure 17, the string length switch is represented as a simple switch. This will be a ticker switch which will click each time the reel spool rotates. In figure 17, there are also four potentiometers used to represent the kite angle sensors. As the resistance of these changes, the input voltage will change telling the microprocessor the angle change of the string. There are two angle sensors for each string, one for vertical angle and one for horizontal angle. Another potentiometer for the tension sensor is used in figure 17. This is a resistor that varies with the pressure placed on it and will be used to find the tension in the kite strings. The voltage and current sensors will be inputs that vary from 0-5 volts. These sensors will take a reading on the voltage and current generated by the generator motor and convert that reading to a 0-5 volt signal. The user interface contains a simple three way switch that will allow the user to select between three modes. The LCD screen will utilize six input/output pins of the microprocessor. The motor controls will utilize six input/output pins as well.

Microprocessor Decision

Criteria	Weights	MicroChip STARTER DEMO BOARD KIT	Futurlec MicroChip Development Board	Individual MicroChip PIC18F4550
Effectiveness	0.4	9	9	8
Practicality	0.2	8	9	7
Time	0.25	8	9	1
Cost	0.15	1	3	9
TOTALS	1	7.35	8.1	6.2

Table 8 - microprocessor selection matrix

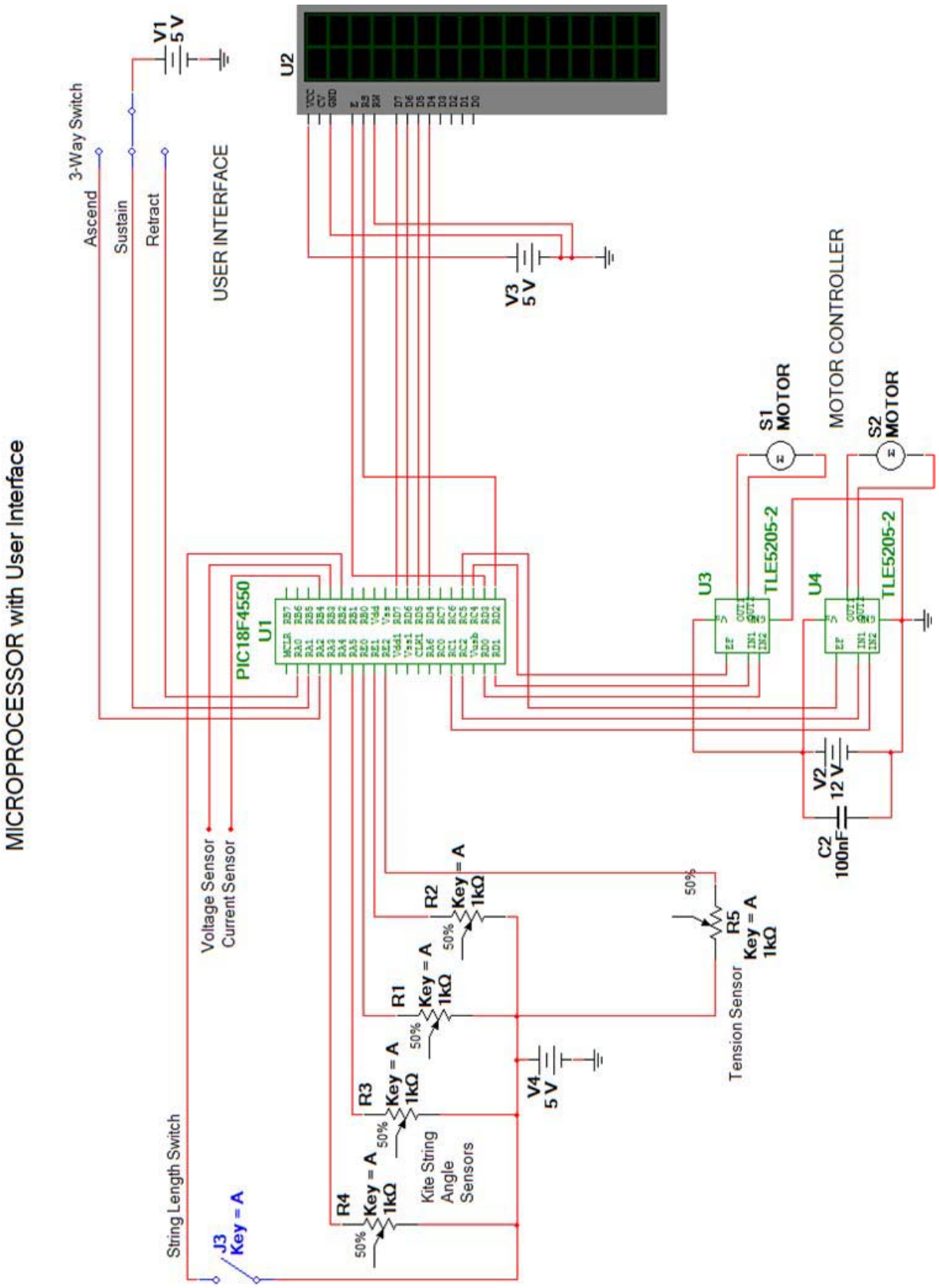

Figure 17 - microprocessor circuit diagram

Software Design

The actual flow of the software is currently becoming more detailed in development. The kite flight test data is still currently being turned into a mathematical model that can easily be manipulated for software applications. All of the sensors will have to be checked on a constant basis and be locked in a continuous loop to keep the kite in flight. The only exceptions will be user-mode changes from the user interface. This switch will trigger interrupts in the microprocessor and alter the flow of the program which will resume once the interrupt is completed. The software system will begin by reading the input A/D ports from the voltage and current sensors to monitor the power generated. It will then calculate the power with an equation programmed into memory. This number will then be stored to memory. The program will then reading the input switch sensor for the kite string and line tension using A/D inputs. These values will then be stored to memory as well. The kite string length and generate power will then be taken out of memory and be translated to allow it to be exported to the LCD screen. The export to the screen will then take place. Once the LCD screen has been updated, the software will begin the check kite algorithm. The software will first read in the values of the kite angle potentiometers and calculate the kite string angles. These angles will then be compared with the kite flight algorithms to determine the next move. These movements will then be applied to the control motors to control the kite. The user three way switch is then checked to see if the kite needs to be retracted or ascended. If it needs to change, an output to the spool motor will be applied. This whole process is then repeated.

Software Flowchart

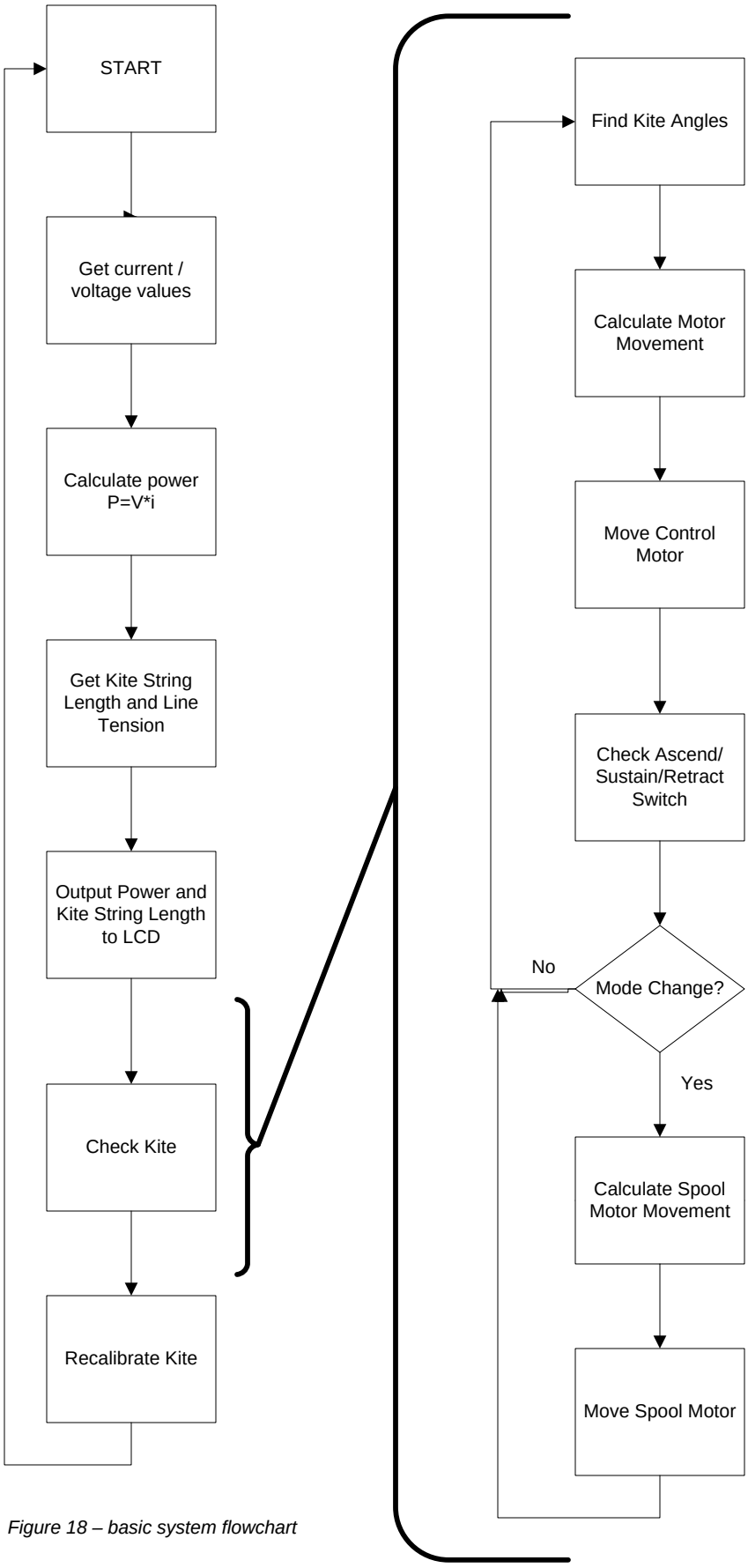

Figure 18 – basic system flowchart

Software Flowchart cont'd

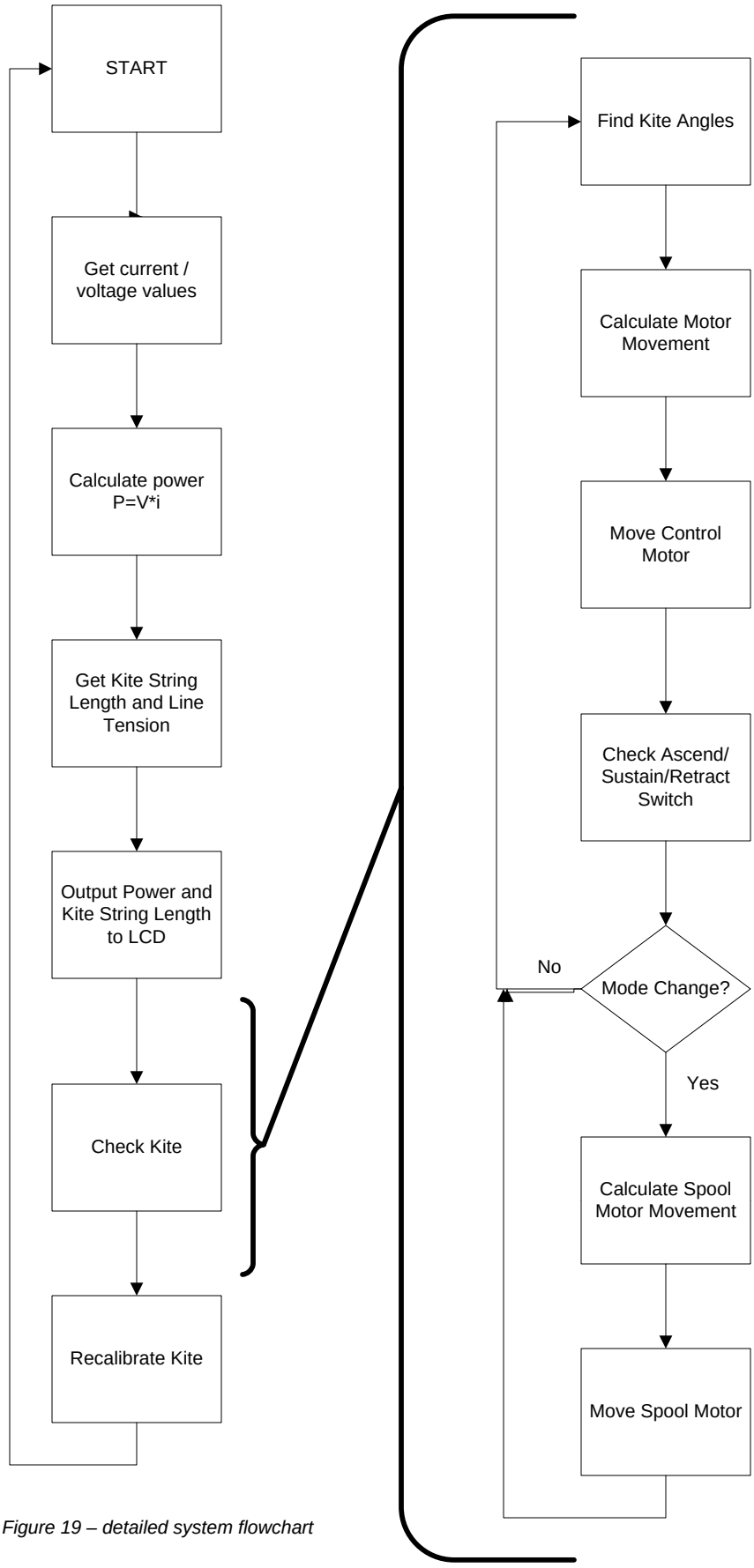

Figure 19 – detailed system flowchart

Motor Controller

Choosing a motor controller configuration is highly dependent upon the types of motors being used. Two different motors need to be chosen for the current project. One motor, the reel motor, will control the spool that allows the kite to ascend, sustain, or retract. The other motor will adjust the kite controls according to the kite control algorithms. The motor chosen for the reel is a typical 12V DC motor, and the control motor is a 1.76V 2A stepper motor that changes at .8 per degree change.

The reel motor will be controlled by an Infineon TLE5205-2 motor controller chip. This chip is a 5A output H-bridge made for DC motor management applications. This chip will accept PWM signals from the microprocessor and will turn the motors on and off based upon the inputs received which are set in the programming of the microprocessor. The motors will not need to vary in speed, only in direction, so only the duration the motor is on will need to be adjusted by the software of the microprocessor.

Functional Truth Table

IN1	IN2	OUT1	OUT2	Comments
L	L	H	L	Motor turns clockwise
L	H	L	H	Motor turns counterclockwise
H	L	L	L	Brake; both low side transistors turned-ON
H	H	Z	Z	Open circuit detection

Table 9 – function truth table of TLE205-2

The control motor can be controller with inputs and outputs from the microprocessor. A set of binary codes are programmed and repeatedly sent to the motor to allow it to move to exact specification. A stepper motor is good for the current application because it allows the system to know exactly how far the controls are moving.

Electrical Components

LCD16x2- 16 x 2 Character LCD Display – *futurlec.com*

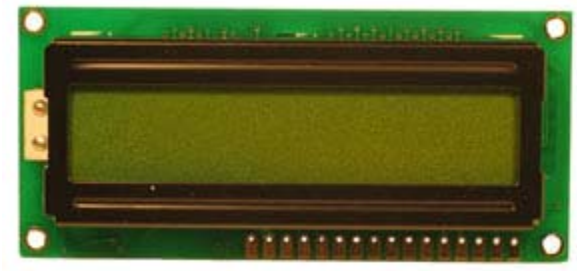

Figure 20 – 16x2 lcd display

Features

- 16 Characters x 2 Lines
- 5 x 7 Dots with Cursor
- Built in Controller
- +5v Power Supply (Also Available for +3V)
- 1/16 Duty Circle

Phidget 30 AMP Current Sensor AC&DC – *trossenrobotics.com*

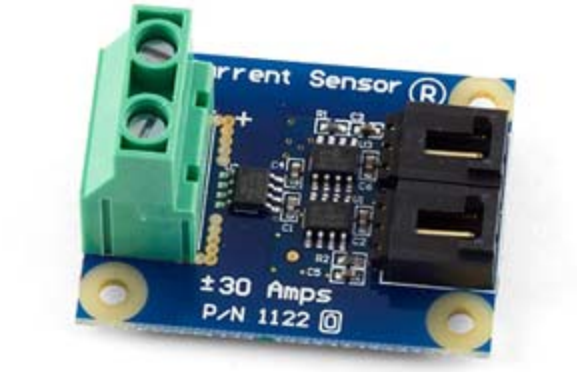

Figure 21 – 30A current sensor

The formula to translate SensorValue into Current is:
DC Amps = (SensorValue / 13.2) - 37.8787
AC RMS Amps = SensorValue x 0.04204

Device Specifications

Characteristic Value
Active Current Consumption 10mA
Output Impedance 1K ohms
Maximum Measurable AC Current 30A
Maximum Measurable DC Current ±30A
Maximum Measurable AC Frequency 10kHz
Current Conductor Resistance 1.5mΩ
Maximum Supply Voltage 5.5VDC
Minimum Supply Voltage 4.5VDC
Terminal Block Recommended Wire Size 10 - 26 AWG
Wire Stripping Length 6-7mm
Total Output Error [1] ±5% Max between -40°C to +85°C
Total Output Error (Typical) ±1.5% @ 25°C

Battery Decision

A large portion of the design decision was reliant upon the battery. The system in creation not only needs to generate power but store it. The chemistry of the battery chosen needs to be looked at closely to make sure it can handle the ruggedness of such a high power system. Since it needs to be a battery that can be recharged, the most likely possible battery chemistries for this system include NiMH, lithium-ion, and lead acid. After analyzing these battery types, a few conclusions can be drawn. NiMH batteries are too small in capacity and are rated at a current too small for the current project. Lithium-Ion batteries would possibly work for the current project but are extremely expensive and would be way out of the budget. The last choice is lead acid which applies satisfactorily to this project. Lead acid batteries are rugged and can handle large voltages and currents. Lead acid batteries (even those rated into the dozens of amp-hours) are moderately affordable. The only disadvantage to lead acid batteries is that a deep discharge can cause an extreme memory loss. The battery chosen is a 12V 26Ah sealed lead acid battery and was purchased for around $50.00.

Access SLAA1224F Battery is rated at 12Volts, 26Ah rating. The Access SLAA1224F Battery from AtBatt.com deliver power when you need it and where you need it. It has been specially designed to meet the power needs of your Access SLAA1224F and is maintenance free, easy to handle, rugged and economical. It has a characteristic of high discharge rate, wide operating temperature, long service life and deep discharge recover.

Amstron 12 volt 26Ah valve regulated sealed lead acid batteries are maintenance free, rugged and economical. Amstron SLA batteries are utilized in a wide variety of applications including electric vehicles, wheelchairs, scooters, UPS backups, computer systems, industrial and medical equipment and more.

Delivering power when you need it, the AP-12260R uses a state of the art, heavy-duty, calcium-alloy grid that provides exceptional performance and service life in both float and cyclic applications.

- *Absorbent Glass Mat (AGM) technology for superior performance*
- *Valve regulated, spill proof construction allows safe operation in any position*
- *High energy density*
- *Approved for transport by air.*
- *UL recognized under file number MH47341*

Specifications

Chemistry	Lead Acid
Voltage	12
Capacity	26,000 mAh / 26 Ah
Rating	312 Whr
Connector	R Terminal
Length	6.54 inch / 16.61 cm
Width	6.89 inch / 17.50 cm
Height	4.92 inch / 12.50 cm
Color	Gray
Weight	18.08 lb / 8,200.91 g
Warranty	1 Year
UPC Code	880487220654

Figure 22 - Amstron 12V / 26Ah Sealed Lead Acid Battery w/ R Terminal

Electronically Assisted Design:

Power from the wind is harnessed from the drag force and movement of the kite parallel to the kite strings through the power generation system. A kite flight pattern that allows the wind to produce this force and movement, thereby transferring power, is necessary. It is also important that this power is delivered in a repeatable method. From the equation for the drag force parallel to the kite strings (equation 1) we see that the force is a function of how much of the kite area is perpendicular to the wind. This renders the power zone as shown is figure 23b where the area, hence forces, are greatest. A kite flying repeatedly in and out of the power zone would produce a figure eight path, such as is shown in figure 23a This path delivers alternating in and out movements that pull the freewheel to generate electricity and then allow the freewheel to be retracted in preparation for another generation pull.

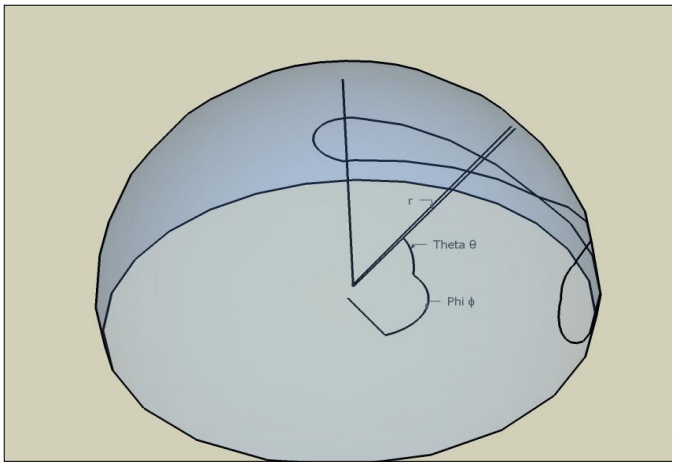

Figure 23a: Sample Flight Path in 3D

Figure 23b: Power Zone

To produce this power generating flight path software, sensors, and electromechanical means will be used. The kite controls sensors will send analog tension sensor and spherical position signals to the microprocessor. The electromechanical controls physically control the kite flight through manipulation of the kite string lengths.

$$F_D = \tfrac{1}{2}\,\rho V^2 C_L A_K$$

Where C_D is the drag coefficient equal to about 1.2, A_K is the kite area $2m^2$, ρ is the density of air at $1.2kg/m^2$, and V is the wind speed.

Controls Sensors Design:

The sensory requirements for autonomous control of the Second Wind system stand on three legs. First the location of kite must be sensed, second the velocity vector of the kite must be sensed, and finally a desired location or path of the kite must be predetermined. The effects of wind speed are discussed below.

The kite's location can be conveniently measured in spherical coordinates using the kite string length for the radius r and sensors attached to the kite strings to sense angles ϕ and θ, as depicted in figure 24, thus giving the kite's location in spherical coordinates.

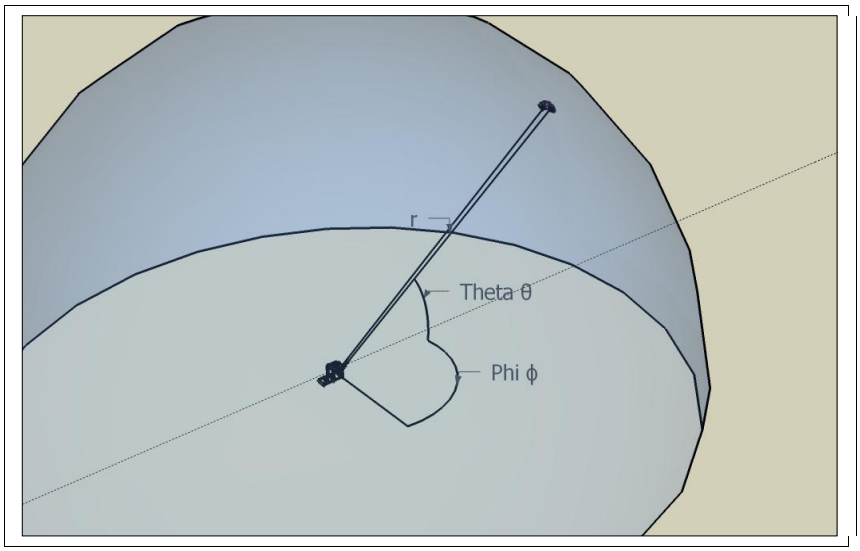

Figure 24: Kite in Spherical Coordinates

Kite velocity vector can be measured by the microprocessor by comparing the change in kite location over time. The accuracy of this method will be affected by the sample rate of the kite location. A single cycle of the flight path was measured to be about 5 seconds with wind speeds around 16 kph (10 mph). If the sample rate is too slow, say 1 Hz, the information is too old to be useful and if the sample rate is too fast, say 10000 Hz, the information will be no more than noise. A tentative sample rate of 40 Hz is proposed giving 200 samples in one cycle. This sample rate will be tested and updated in the future. Lastly the predetermined path shall be a flight pattern's coordinates that are stored in the microprocessor. In order for this pattern to be useful in variable wind conditions it must be scaled in real time proportional to wind speed.

Two options for location/velocity sensors were compared using a decision matrix as shown in Table 25.

Attribute	**Weight**		**Potentiometer**	**Inclinometer**
Cost	40.00%		*10	5
Simplicity	40.00%		7	6
Reliability	20.00%		7	10
Total	100.00%		82.00%	64.00%

Table 10: Location/Velocity Sensor Decision Matrix.
*NOTE: Ratings are on a 0 to 10 scale where 0 is least desirable and 10 is the most.

A test mock up of the potentiometer sensor was made and its applicability was established. The test platform was constructed using two potentiometers, various lego parts, and two protractors such that the Θ and Φ angles of a single angle arm could be measured. This test platform is depicted in Figure 25 below.

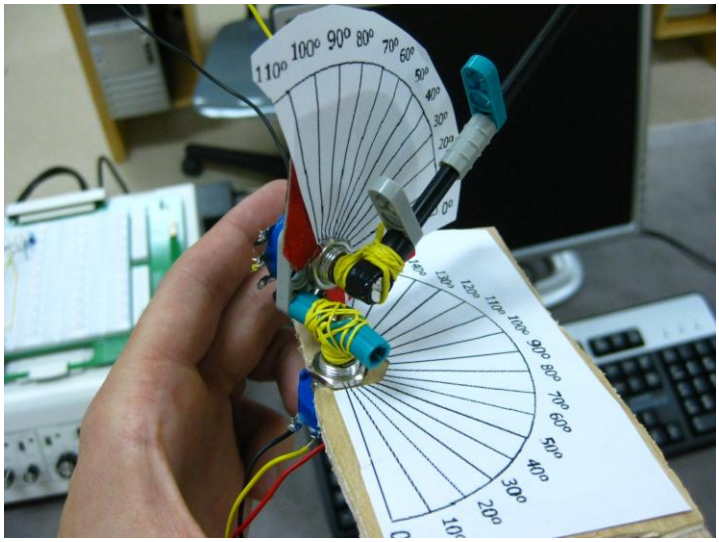

Figure 25 Test platform

Samples of the Φ potentiometer's resistances at the angles 0,10,20,30 on until 180 degrees were taken, recorded, and graphed. Similarly, samples of the Θ potentiometer were taken at angles 0,10,20,30 on until 110 degrees were taken, recorded, and graphed. Trend lines for each graph were made.

Using the equations generated by the trend lines a program was written in LabView to convert the measured resistance to an angle measuring device in LabView.

The resulting graphs are shown in Figure 26 and Figure 27 below.

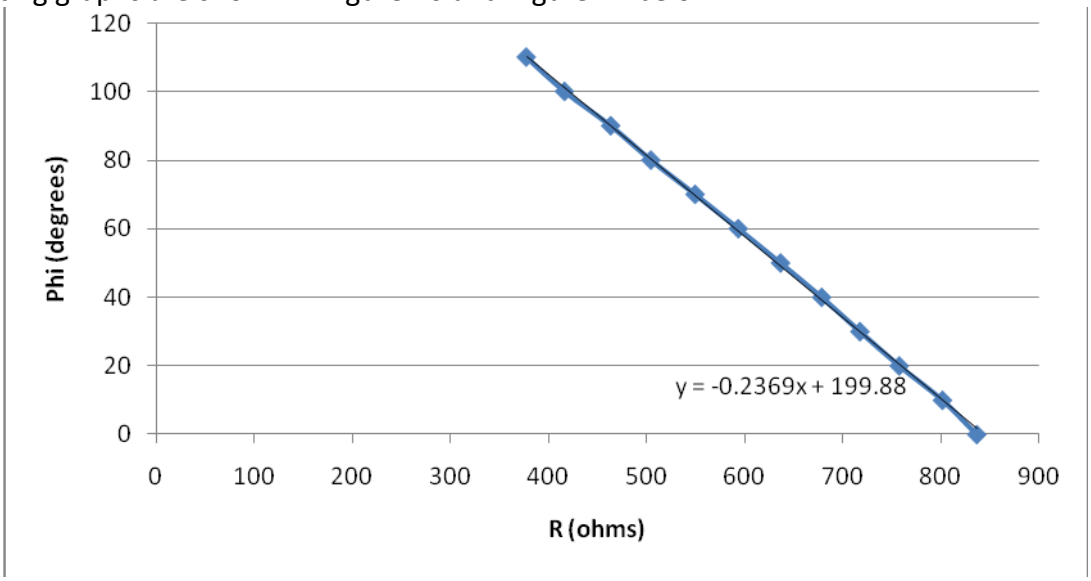

Figure 26: Phi vs R

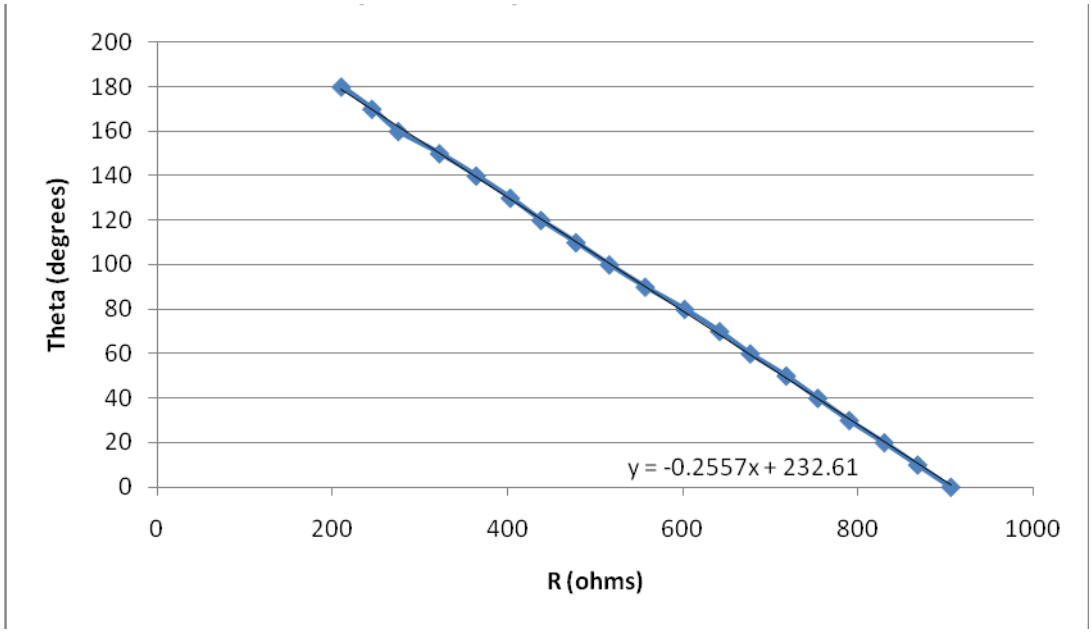

Figure 27: Theta vs R

The results of the program written in LabView for Phi are shown in Figure 28 and the results for Theta are in Figure 29 below.

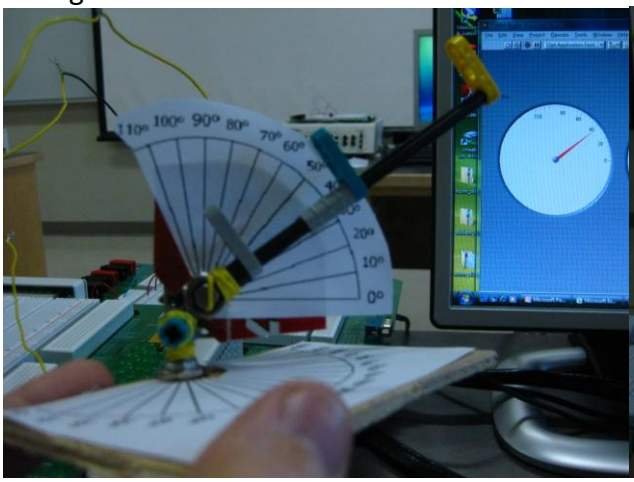

Figure 28 Results for Theta

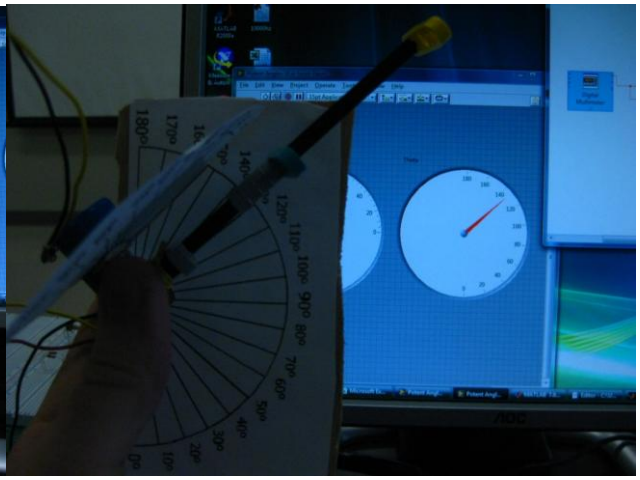

Figure 29 Results for Phi

From Figures 26 and 27 we can see that the resistance change with angle is in fact linear. This fact is confirmed by the angles indicated in the LabView program output seen in Figures 28 and 29. The angles read using the program were close if not identical to those observed on the test platform. The pros of this method of measuring the Θ and Φ are that it is relatively inexpensive and easy to construct. Possible cons of this method are that is it mechanically intensive (could have problems with dust, rust, etc. There could also be a problem with drift depending on the quality of the potentiometer used.

This is a very good potential method of measuring the angles of the kit strings provided dust, rust and drift are considered in the design.

The total cost for this sensor design is estimated to be between $3 and $5 each and falls under the miscellaneous electronics category in the budget.

In order to scale the predetermined flight pattern proportional to wind speed a tension sensor was designed. Actual wind speed was not sought because the tensions on the line could be used to represent both the wind speeds and serve in testing for the efficiency of the overall system. The force sensor selected for our tension sensor, shown in figure 30, will be incorporated into an overall design as shown in figures 31 and 32.

8" FlexiForce 0-100 lbs. Resistive Force Sensor Kit:

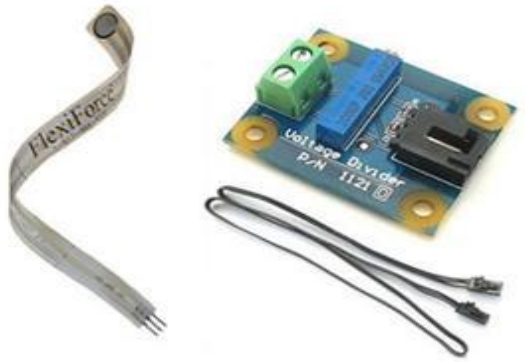

- 0-100 lbs FlexiForce Force Sensor
- Phidget Voltage Divider
- 24" Sensor Cable
- Price: $24.40

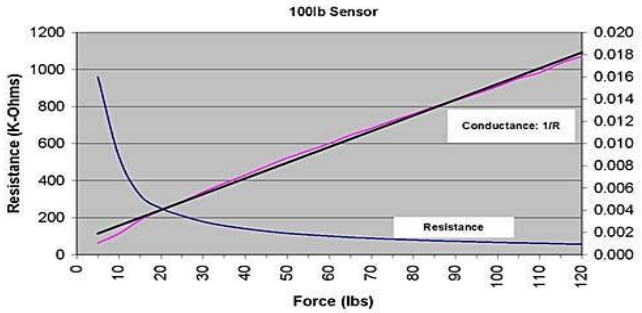

Figure 30: Force Sensor Kit

The tension sensor design shown in figure 32 converts the tension on the string to a force on the FlexiForce sensor.

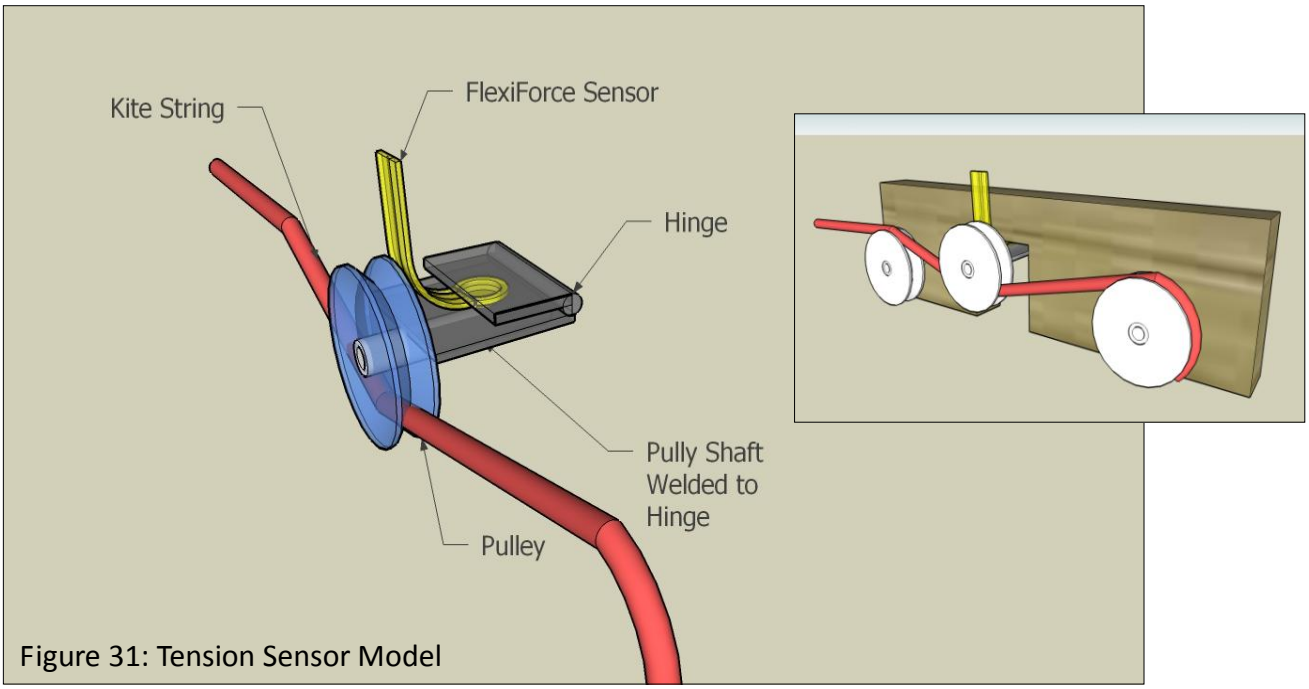

Figure 31: Tension Sensor Model

The tension on the string can be calculated from the force measured on the FlexiForce sensor as shown in the following equation.

$$T = (A*Fs)/[(A+B)*\sin(\lambda)]$$

Where T is the tension on the string and Fs is the measured force on the sensor. The dimensions A, B, and λ will be considered constant and are to be measured as shown in figure 32.

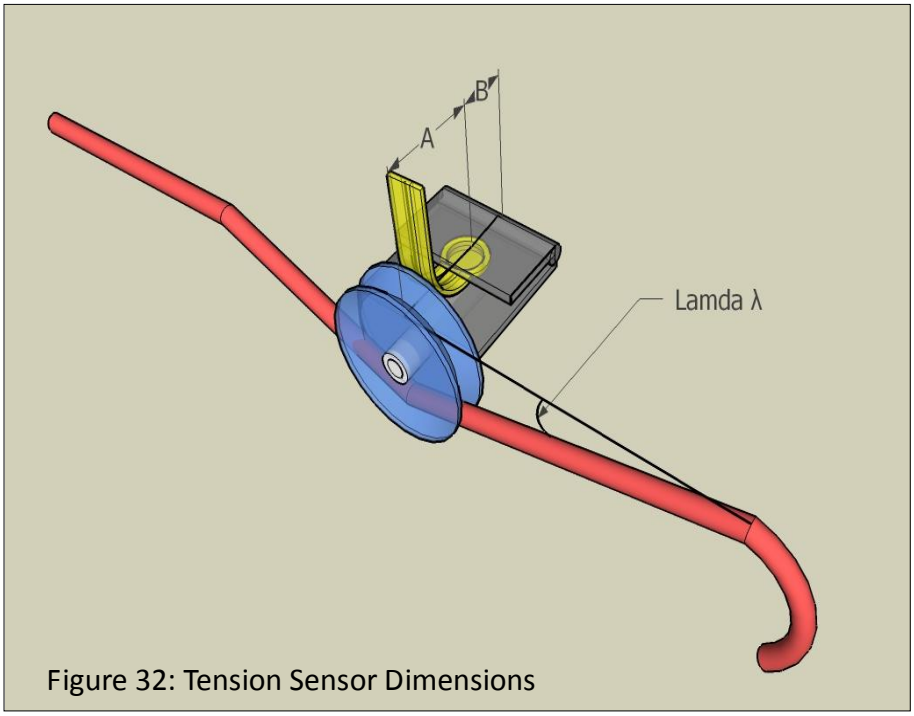

Figure 32: Tension Sensor Dimensions

A figure eight flight path was chosen because it readily delivered the repetitive power zone enter and exit pattern. As was stated previously, the path should be scaled with wind speed. A depiction of such a path is shown in figure 23a.

This path is ideal because of the power zone shown previously in figure 23b. The kite flies into the red power zone delivering maximum tension, pulling the freewheel and generating electricity. Next the kite flies into the low tension light blue zone allowing the free wheel to retract, the kite loops back and the process is repeated.

Controls Kite String Manipulator Design:

The kite's flight is manipulated by pulling the right line IN while letting the left line OUT to turn CW and pulling the left line IN while letting the right line OUT to turn CCW. To accomplish this a slider controller is designed such that the linear movement of the slider causes the above mentioned maneuvers. Our designed controller is depicted in figure 33.

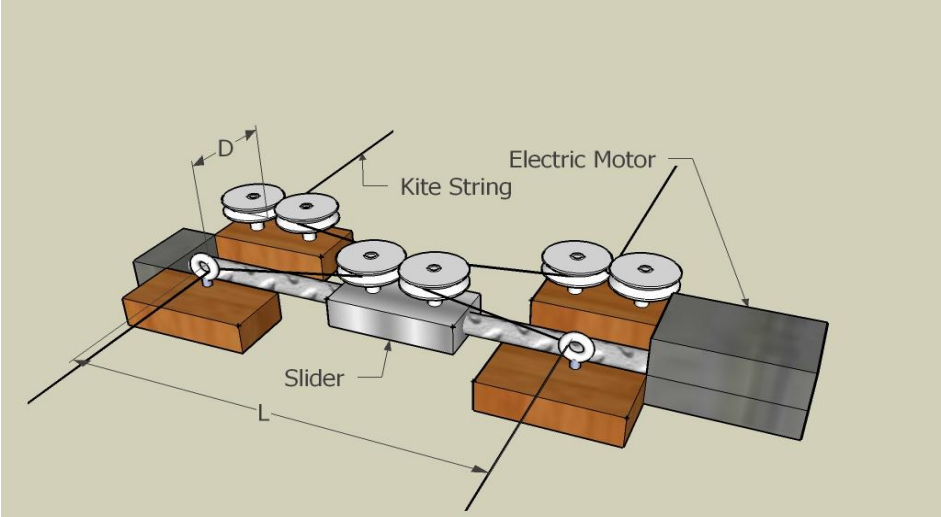

Figure 33: Slider Controller Design

The slider controller is depicted from above in figure 34. It can be seen that when theta equals zero the line length Y can be calculated to be equal to twice that of the slider position X. For example, as the slider moves distance X to the right, the right line will bet let out distance 2*X and the left line will be taken in distance 2*X. The converse is true of the slider moving to the left. This effectively

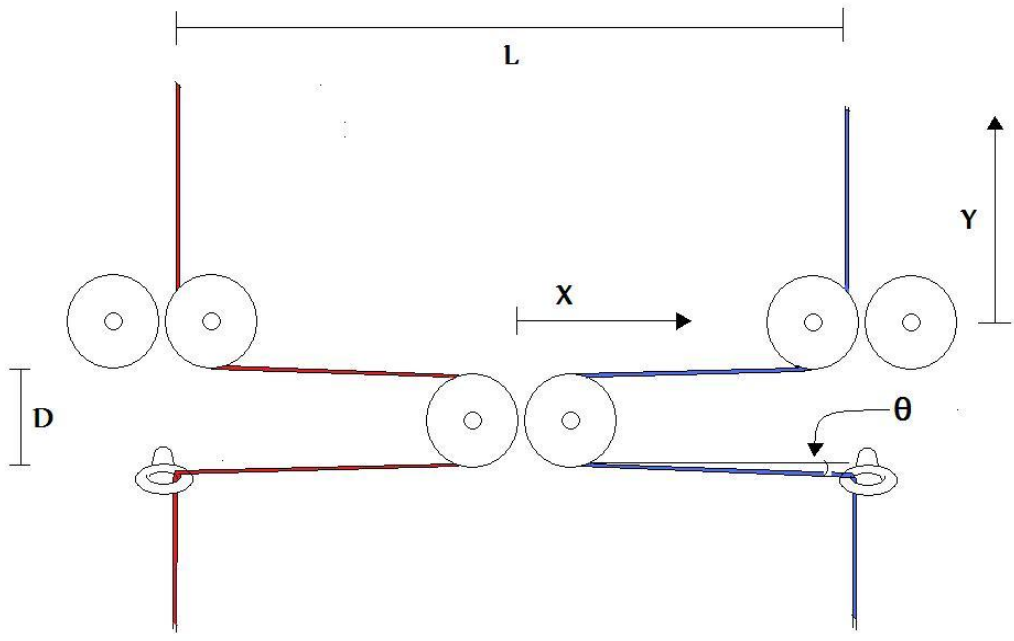

Figure 34: Slider Controller Design From Above

turns the kite. This design is particularly advantageous as line tensions increase because the tensions will, for the most part, cancel each other leaving the majority of the power required to move the control slider. This is only valid as the angle θ approaches zero so that the distance D between the eye hole and the side pulley is the same as the diameter of the central pulleys. The length of a standard kite control bar is 50cm. The most extreme turning angle achievable with this control bar is reached when the bar is parallel with the kite string. That is to say one side of the bar has been pulled away from the kite to the the max and the other has been pushed out towards the kite to the max. The change in line length during this maneuver is exactly 25cm for each side. This tells us that the maximum change in line length needed to control the kite is 25cm. Therefore the length (L) for our slider design must have a minimum of 25cm or roughly 9.9in to sufficiently control the kite. The difference in the forces on the slider is the difference in the line tensions doubled.

To determine the difference in the line tensions during a turn we must understand the dynamics taking place during the kite's flight. In figure 35 we see a free body diagram of the kite with the control slider at neutral. The wind is assumed to be parallel to the ground thereby causing drag force normal to the inside of the kite. We can see that, because of the slightly tiled orientation of the kite to the wind, the component of the drag force in the ***y*** direction must cause acceleration of the kite in an ark about the ***z*** direction. As the kite flies forward we also see a lift force acting due to the parafoil shape.

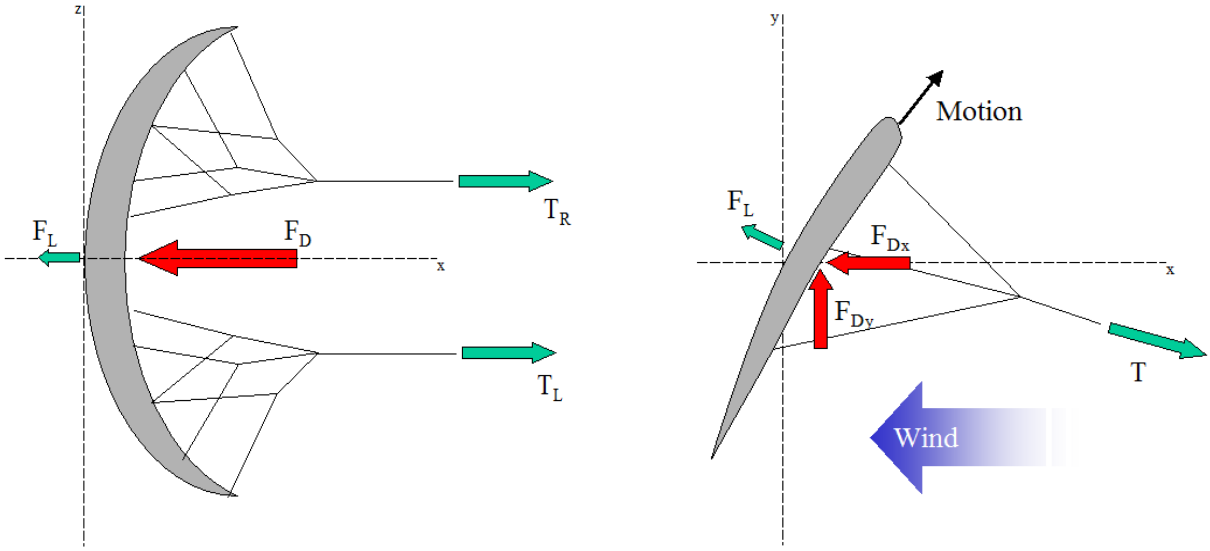

Figure 35: Kite FBD With Control Slider at Neutral

In figure 36 we see an example of a right turn. When the slider is moved to the left the right string is retracted and the left string is given slack. This re-orients the kite to the wind such that the drag force normal to the kite now has a component along the ***z*** axis. The aerodynamic design of the kite causes the kite to turn about the ***x*** axis as is moves along the ***z*** axis.

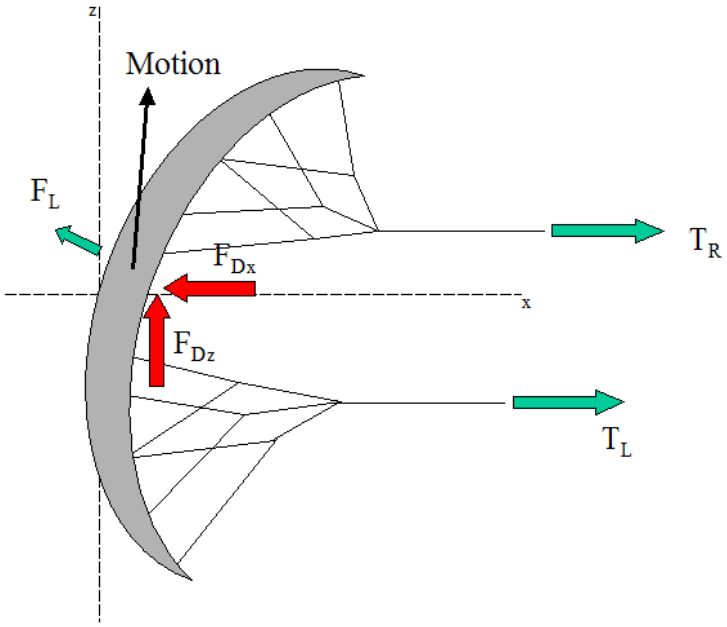

Figure 36: Kite FBD With Right Turn

If we assume that the drag force and lift force along the ***x*** axis are at the center of the kite, that the kite strings are at an equal distance R_{center} from the center, and that there is no movement in the x direction then we can say from statics that T_R and T_L are equal and there is no difference in line tension.

$$\Sigma My: \; T_L*R_{center} + T_R*R_{center} = 0$$

Therefore we can say that there will be no holding force needed. The work required to make the line length change can be calculated as the difference of the work done by the slider to pull one line in and the work done on the slider by the other line going out.

$$W_{total} = F_S*x - T_L*x*2$$

From the free body diagram in figure 37 we can see that

$$F_S - 2*T_R - F_{Friction} = M_{system}*a_{slider}\ .$$

Plugging this into the work equation we get

$$W_{total} = (2*T_R + F_{friction} + M_{system}*a_{slider})*x - T_L\,x*2$$

Assuming $T_R = T_L$ this can simplify to

$$W_{total} = (F_{friction} + M_{system}*a_{slider})*x$$

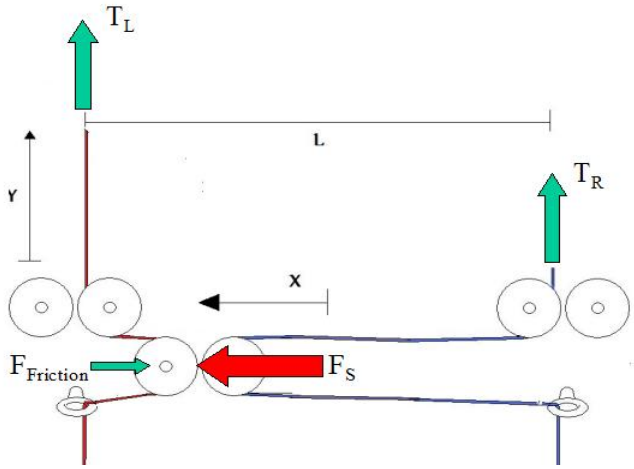

Figure 37: Slider Controller FBD

We see that the amount of work done by the slider will primarily be a function of friction in the system and the mass and acceleration of the system. It can be assumed that any slider purchased will already be able to move its own weight. The only other mass in this system is that of the kite and the strings which are negligible. In conclusion; special attention to the frictional losses to be overcome by the controller must be considered in the final selection of small parts that the strings run through such as pulleys and eye holes.

The current slider design is made of the components shown in figure 38.

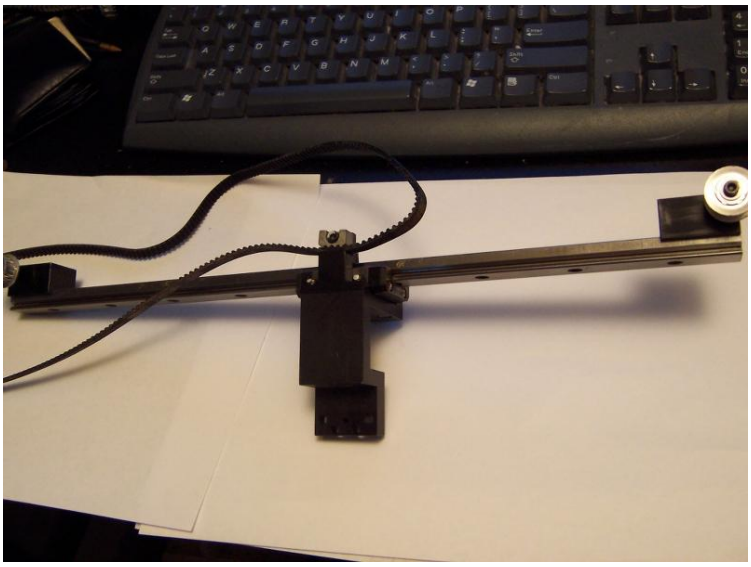

Belt Slider Rail

Truck travel: 13 inches
Cost: $45 (including shipping)

Figure 38: Belt Slider Rail

A motor was purchased to run this slider. The motor is rated at 1.76V 2A and turns at 0.8 deg per revolution. A cog pulley came with the motor that will mate with the belt drive. This motor coasted $35 with shipping. This slider meets the length requirements of a 9.9 inch travel length.

Kite Retraction System Design:

The purpose of the kite retraction system is to deploy and retract the kite when the user so desires or to retract the kite when wind speed is either too high for safety or too low for flight >50 kph <6 kph.

Two designs were considered, one using a motorized big game fishing reel, and the other using a simple motor and drum set up. A decision matrix was created to help in the decision process and is shown in table 11.

Attribute	**Weight**		**Fishing Reel**	**Simple Drum**
Cost	50.00%		*6	10
Simplicity	30.00%		7	10
Consistent Line Intake	20.00%		10	7
Total	100.00%		71.00%	94.00%

Table 11: Kite Retraction Decision Matrix.
*NOTE: Ratings are on a 0 to 10 scale where 0 is least desirable and 10 is the most.

As is shown above the decision was made to go with a simple drum. In the design specifications the retraction time is set to be no less than 10 minutes. Using equation 3 it has been

calculated that the maximum rated tension on the kite during retraction (when the only force on the kite will be due to lift) is equivalent to 28.13 N rounded up (about 7lb). A spreadsheet, shown in table 12 was made to find the appropriate spool dimensions, rpm, and torque for these requirements.

$$F_L = \tfrac{1}{2}\,\rho V^2 C_L A_K$$

Where C_L is the lift coefficient equal to about 0.15, A_K is the kite area $2m^2$, ρ is the density of air at $1.2kg/m^2$, and V is the wind speed.

	A	B	C
1	**Independent Variables:**		
2	Voltage to Motor (V)	6	
3	String Lenth (ft,m)	90	27.43
4	Retraction Time (min)	5	
5			
6	**Dependent Variables:**		
7	Design Radius of Spool (in,cm)	0.56	1.42
8	Amps to Motor	21.85	
9	Whr output to reel in	12.02	
10			
11	rate line in (ft/min,m/min)	18.00	5.49
12	rate spool spin (rev/min)	2658.00	
13	length per revolution(ft,cm)	0.01	0.21
14	torque needed (lb*in,N*cm)	3.52	39.81

Table 12: Excel spreadsheet screen shot.

The equations used to calculate the values in table 12 are as listed below:

Rate line in = string length/retraction time

Rate spool spin = Voltage to Motor * 443rpm/V -> from CIM motor specks

Length per revolution = Rate line in / Rate spool spin

Design Radius of Spool = sqrt(Length per revolution/[pi*12])

Torque Needed = Design Radius of Spool * 7 lb

Amps to Motor = Torque needed / 0.16124 lb*in/A -> from CIM motor specks

These values were then converted to metric units as well.

The retraction time value was set to five minutes instead of the required ten minutes in order to design for a factor of safety of two. Using this spreadsheet a motor was found that met the specified requirements. The specific motor selected is shown in figure 43 and the resulting system using this motor is shown in figure 44. It can be calculated that at most about 12.77 watt hours is required to deploy and retract the kite.

$$Wh_{total} = [Wh_{deploy} = 6v*2.7A*(2.5/60)hr] + [Wh_{retract} = 6v*24.19A*(5/60)hr] = 12.77\ Wh$$

This is insignificant because in the event of a case where wind speeds are high enough to produce such lift forces on the kite the power generated due to those same high winds would offset any losses due to the retraction of the kite.

FIRST CIM Motor:

- Operating v : 6v - 12v
- Nominal v : 12v
No Load RPM : 5310
No Load A : 2.7A
Stall Torque : 343.27 oz-in 2424 mN-m
Stall Current : 133A
Kt : 2.58 oz-in/A 18.2 mN-m/A
Kv : 443 rpm/V
Efficiency : 65%
RPM - Peak Eff: 4614
Torque - Peak Eff : 45 oz-in/A 317.8 mN-m
Current - Peak Eff : 19.8A

Figure 39: Retraction Motor

The kite reel system will also act as the kite break system. The cost of parts for the spool drum will be insignificant due to the fact that its parts can be found in a common junk yard or even made out of PVC pipe. The value of the spool will be recorded in our records but budget will not suffer.

Figure 40: Retraction System

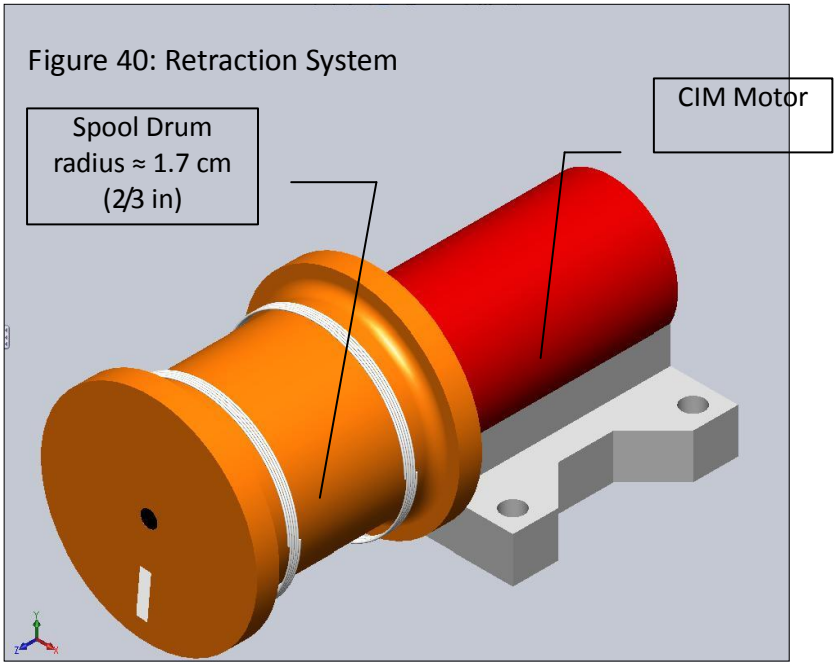

Budget Analysis

Currently 33.3% of the budget has been used by spending $283.09. A large number of purchases will be made within the next week so that majority of the required parts for the system will be purchased. Vendors have been selected for all the parts of the project.

Some of the more expensive items:

- Kite
- Generator Motor
- Development Board
- Battery

These are some of the more important items that were required in order to further the research and development of the project.

The generator motor was expected to be more expensive, so this was an unexpected saving. The budget previously listed the use of used bicycle parts for items such as sprockets, chains, and axles. However, the design now calls for the use of sprockets and chains of different pitch from a bicycle system. However, due to the low cost of the motor, the sprockets and chains still fit within the budget of the generation system.

The battery design was changed from one that could hold 500 watt hours of energy to one that can hold just over 300 watt hours of energy. This design change was done in order to save on the cost of the battery. The system will still be able to show that it can produce 500 watt hours of energy within a ten hour period.

A development board was purchased instead of individual microprocessors to allow for ease and speed of programming. The change proved more expensive however, the microprocessor that comes with the development board has free samples that can be obtained.

Another major change to the budget comes from the controls system. It was determined that the most accurate and effective way to control the kite would be by using a system similar to that used on computer numerical control (CNC) machines. These slider controller mechanisms can be purchased on ebay, however they are expensive, and will therefore be a larger part of our budget.

The updated budget has allocated $91.82 or 10.80% of the total budget as a buffer in case of unpredicted expenditures in the future. So, as of now the project is still on budget.

Updated Budget			
Product	**Vendor**	**Cost**	**Ordered**
Kite	Kite Wind Surf	$131.95	Y
Development Board	Futurlec	$52.90	Y
Battery	atbatt.com	$50.33	Y
Generator Motor	Monster Scooter Parts	$47.91	Y
Nuts/Bolts/Wood	Lowes	$50.00	
Sprockets/Chains/Axle	Electric Scooter Parts	$104.87	Y
Axle	Lowes	$5.71	
Springs	W.B. Jones Spring Co.	$36.00	Y
Bearings	VXB.com	$28.43	Y
Circuit Boards	4pcb	$50.00	
Controls System	ebay.com	$80.00	Y
Retraction Motor	Trossen Robotics	$32.00	Y
Sensors	Trossen Robotics	$78.62	Y
Electrical Components	allelectronics.com	$25.00	
Miscellaneous		$76.28	
TOTAL		$850.00	
Amount Spent		$643.01	
80% of Budgeted Items		$618.98	

Figure 41

Schedule Analysis

Having a retrospective look at our semester has given us essential insight for the remainder of our project's development. After the completion of our Requirements Specification our project was well under way. Research began to become more intensive and creativity was vital. As we continued to meet deadlines, our first accomplishment was the successful delivery of our Stage/Gate Presentation as well as the completion of our Final System Overview and Project Plan. Once this was completed, deadlines became more reliant upon the timeframes our own group established. We are persisting through the final steps in the design process.

Hands-on models, circuit simulations and schematics, 3-D Solidworks models and analyses, and overall systems analyses have been completed. Analyses of Solidworks models and circuit diagrams have taken place in order to justify our design choices. There are currently still finalizations being made to a few subsystems but this should not cause many future delays. These finalizations begin with the kite control algorithms. A little behind schedule, the algorithms are still being modeled in a way that is applicable for software development. This should be finished by the end of the semester but can be finished during the first week of Christmas break if needed. A final decision on the control motor also still needs to be made. The limitations in variety, voltage/current necessities, and funds are making this a difficult search, but it will be decided and ordered by the end of the fall semester. This decision is slightly delaying the design for the motor controller since motor specifications for the control motor are not yet available, only assumptions can be made. Thankfully, the motor controller configuration is simplistic and will be quick and easy to implement (less than a week) once a motor decision is made. This final motor controller design implementation may need to take place over Christmas break, but the spring semester will not be delayed. More research is also being done in the use of the microprocessor in order to begin programming. The microprocessor wasn't received until December 8, 2009, so strides toward being able to program are well under way. More microprocessor self-education and programming will take place over Christmas break and will allow the spring semester to run smoothly from a software standpoint. Any delays are only minor design decisions that can be decided before the spring semester. Parts selection is still taking place, however all parts will be ordered before Christmas break and are expected to arrive by January 11. Final analyses and simulations are being completed for use in the final presentation.

Gantt Chart - Fall 2009

Second Wind

Josh Dowler, Caleb Meeks, John Snyder

ID	Task Name	Start Date	Finish Date	Duration (Weeks)
F1.0	**Requirements Specifications**	9/8/2009	9/29/2009	3
F2.0	**System Overview**	9/8/2009	10/13/2009	4
F3.0	**Controls Design**	9/29/2009	11/17/2009	7
F3.1	Mechanically Governed System Design	9/29/2009	10/20/2009	3
F3.2	Electronically Assissted Design	10/27/2009	11/17/2009	3
F3.3	Kite Retraction System Design	10/13/2009	10/27/2009	2
F3.4	Brake System Design	10/20/2009	10/31/2009	1.5
F4.0	**Generator Design**	9/29/2009	11/10/2009	5
F4.1	Freewheel and Return Design	10/20/2009	11/10/2009	3
F4.2	Gearing Ratio Design	10/13/2009	10/27/2009	2
F4.3	Generator Motor Selection	9/29/2009	10/20/2009	3
F5.0	**Charge Controller Design**	9/29/2009	10/13/2009	2
F6.0	**Motor Controller Design**	10/6/2009	10/27/2009	3
F7.0	**Microprocessor Interface Design**	10/13/2009	11/3/2009	3
F8.0	**User Interface Configuration Design**	11/3/2009	11/14/2009	1.7
F9.0	**System Frame Design**	11/3/2009	11/10/2009	1
F10.0	**Parts Selection**	9/26/2009	11/10/2009	6.5
F11.0	**System Analysis**	11/17/2009	12/7/2009	1.7
F12.0	**System Design / Project Plan**	10/1/2009	10/13/2009	1.4
F13.0	**Final Design**	11/17/2009	12/8/2009	1.8
A1.0	**Documentation**	9/8/2009	12/10/2009	12.5
A2.0	**Project Management**	9/8/2009	12/10/2009	12.5

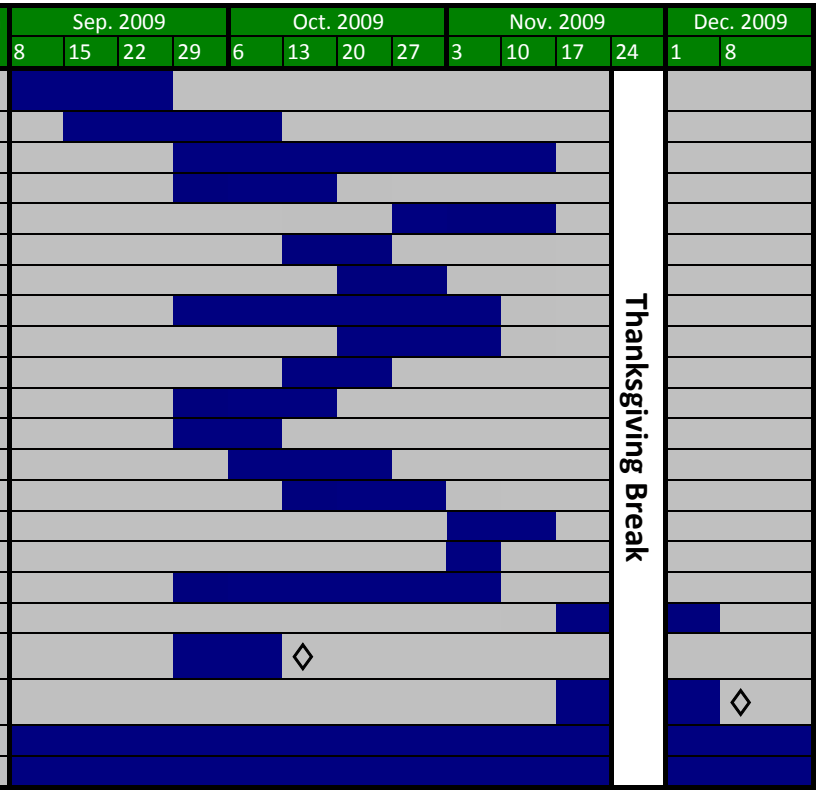

Figure 42

Gantt Chart - Spring 2010

Second Wind

Josh Dowler, Caleb Meeks, John Snyder

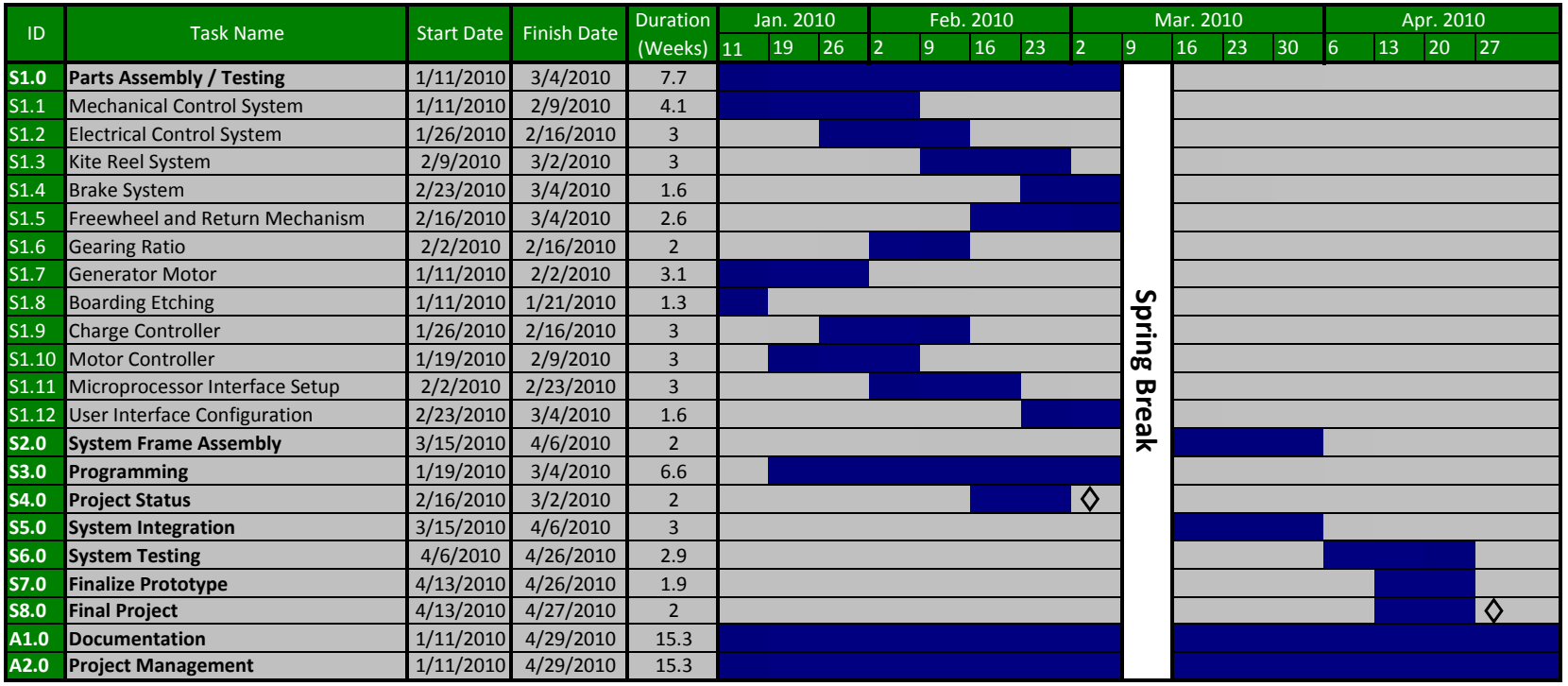

ID	Task Name	Start Date	Finish Date	Duration (Weeks)
S1.0	**Parts Assembly / Testing**	1/11/2010	3/4/2010	7.7
S1.1	Mechanical Control System	1/11/2010	2/9/2010	4.1
S1.2	Electrical Control System	1/26/2010	2/16/2010	3
S1.3	Kite Reel System	2/9/2010	3/2/2010	3
S1.4	Brake System	2/23/2010	3/4/2010	1.6
S1.5	Freewheel and Return Mechanism	2/16/2010	3/4/2010	2.6
S1.6	Gearing Ratio	2/2/2010	2/16/2010	2
S1.7	Generator Motor	1/11/2010	2/2/2010	3.1
S1.8	Boarding Etching	1/11/2010	1/21/2010	1.3
S1.9	Charge Controller	1/26/2010	2/16/2010	3
S1.10	Motor Controller	1/19/2010	2/9/2010	3
S1.11	Microprocessor Interface Setup	2/2/2010	2/23/2010	3
S1.12	User Interface Configuration	2/23/2010	3/4/2010	1.6
S2.0	**System Frame Assembly**	3/15/2010	4/6/2010	2
S3.0	**Programming**	1/19/2010	3/4/2010	6.6
S4.0	**Project Status**	2/16/2010	3/2/2010	2
S5.0	**System Integration**	3/15/2010	4/6/2010	3
S6.0	**System Testing**	4/6/2010	4/26/2010	2.9
S7.0	**Finalize Prototype**	4/13/2010	4/26/2010	1.9
S8.0	**Final Project**	4/13/2010	4/27/2010	2
A1.0	**Documentation**	1/11/2010	4/29/2010	15.3
A2.0	**Project Management**	1/11/2010	4/29/2010	15.3

Figure 43

Appendices

Appendix A

MAX15046 DC-DC Converter

19-4719; Rev 0; 7/09

40V, High-Performance, Synchronous Buck Controller

General Description

The MAX15046 synchronous step-down controller operates from a 4.5V to 40V input voltage range and generates an adjustable output voltage from 85% of the input voltage down to 0.6V, supporting loads up to 25A. The device allows monotonic startup into a prebiased bus without discharging the output and features adaptive internal digital soft-start.

The MAX15046 offers the ability to adjust the switching frequency from 100kHz to 1MHz with an external resistor. The MAX15046's adaptive synchronous rectification eliminates the need for an external freewheeling Schottky diode. The device also utilizes the external low-side MOSFET's on-resistance as a current-sense element, eliminating the need for a current-sense resistor. This protects the DC-DC components from damage during output overloaded conditions or output short-circuit faults without requiring a current-sense resistor. Hiccup-mode current limit reduces power dissipation during short-circuit conditions. The MAX15046 includes a power-good output and an enable input with precise turn-on/turn-off threshold, which can be used for input supply monitoring and for power sequencing.

Additional protection features include sink-mode current limit, and thermal shutdown. Sink-mode current limit prevents reverse inductor current from reaching dangerous levels when the device is sinking current from the output.

The MAX15046 is available in a 16-pin QSOP or 16-pin QSOP-EP package and operates over the -40°C to +125°C temperature range.

Pin Configurations appear at end of data sheet.

Features

- **Input Voltage Ranges from 4.5V to 40V or 5V ±10%**
- **Adjustable Outputs from 0.85 x V_{IN} Down to 0.6V**
- **Adjustable Switching Frequency (100kHz to 1MHz) with ±10% (1MHz) Accuracy**
- **Adaptive Internal Digital Soft-Start**
- **Up to 25A Output Capability**
- **Cycle-by-Cycle Valley-Mode Current Limit with Adjustable, Temperature-Compensated Threshold (30mV to 300mV)**
- **Monotonic Startup into Prebiased Output**
- **±1% Accurate Voltage Reference**
- **3A-Peak Gate Drivers**
- **Hiccup-Mode Short-Circuit Protection (Patent-Pending Architecture)**
- **Overtemperature Shutdown**
- **Power-Good (PGOOD) Output and Enable Input (EN) with ±5% Accurate Threshold**
- **Thermally Enhanced 16-Pin QSOP Package**

Applications

Industrial Power Supplies (PLC, Industrial Computers, Fieldbus Components, Fieldbus Couplers)

Telecom Power Supplies

Base Stations

Ordering Information

PART	TEMP RANGE	PIN-PACKAGE
MAX15046AAEE+	-40°C to +125°C	16 QSOP
MAX15046BAEE+	-40°C to +125°C	16 QSOP-EP*

+Denotes a lead(Pb)-free/RoHS-compliant package.

**EP = Exposed pad.*

Typical Operating Circuit

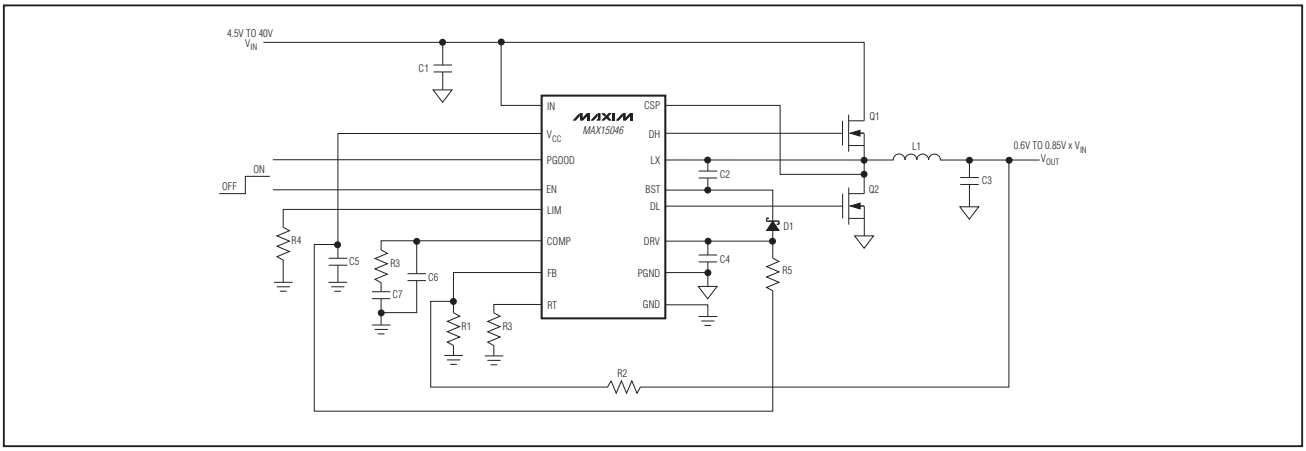

For pricing, delivery, and ordering information, please contact Maxim Direct at 1-888-629-4642, or visit Maxim's website at www.maxim-ic.com.

40V, High-Performance, Synchronous Buck Controller

ABSOLUTE MAXIMUM RATINGS

IN to GND ..... -0.3V to +45V
V_{CC} to GND ..... -0.3V to lower of (V_{IN} + 0.6V) and 6V
EN, DRV to GND ..... -0.3V to +6V
PGOOD to GND ..... -0.3V to +45V
PGND to GND ..... -0.3V to +0.3V
DL to PGND ..... -0.3V to (V_{DRV} + 0.3V)
BST to PGND ..... -0.3V to +50V
LX and CSP to PGND ..... -1V to +45V
LX and CSP to PGND ..... -2V (50ns max) to +45V
BST to LX ..... -0.3V to +6V
CSP to LX ..... -0.3V to +0.3V
DH to LX ..... -0.3V to (V_{BST} + 0.3V)
All Other Pins to GND ..... -0.3V to (V_{CC} + 0.3V)
V_{CC} Short Circuit to GND ..... Continuous
PGOOD Maximum Sink Current 20mA

Continuous Power Dissipation (T_A = +70°C):
16-Pin QSOP (derate 9.6mW/°C above +70°C) 771.5mW
16-Pin QSOP-EP (derate 22.7mW/°C above +70°C) 1818.2mW
Junction-to-Case Thermal Resistance (θ_{JC}) (Note 1)
16-Pin QSOP ..... 37°C/W
16-Pin QSOP-EP ..... 6°C/W
Junction-to-Ambient Thermal Resistance (θ_{JA}) (Note 1)
16-Pin QSOP ..... 103.7°C/W
16-Pin QSOP-EP ..... 44°C/W
Operating Temperature Range ..... -40°C to +125°C
Junction Temperature ..... +150°C
Storage Temperature Range ..... -65°C to +150°C
Lead Temperature (soldering, 10s) ..... +300°C

Note 1: Package thermal resistances were obtained using the method described in JEDEC specification JESD51-7, using a four-layer board. For detailed information on package thermal considerations, refer to **http://www.maxim-ic.com/thermal-tutorial**.

Stresses beyond those listed under "Absolute Maximum Ratings" may cause permanent damage to the device. These are stress ratings only, and functional operation of the device at these or any other conditions beyond those indicated in the operational sections of the specifications is not implied. Exposure to absolute maximum rating conditions for extended periods may affect device reliability.

ELECTRICAL CHARACTERISTICS

(V_{IN} = 24V, V_{EN} = 5V, V_{GND} = V_{PGND} = 0V, C_{IN} = 1µF, C_{VCC} = 4.7µF, R_{RT} = 49.9kΩ, T_A = T_J = -40°C to +125°C, unless otherwise noted. Typical values are at T_A = +25°C.) (Note 2)

PARAMETER	SYMBOL	CONDITIONS	MIN	TYP	MAX	UNITS
SYSTEM SPECIFICATIONS						
Input-Voltage Range	V_{IN}		4.5		40	V
		V_{IN} = V_{CC} = V_{DRV}	4.5		5.5	
Quiescent Supply Current	I_{IN_Q}	V_{IN} = 24V, V_{FB} = 0.9V, no switching		2	3	mA
Shutdown Supply Current	I_{IN_SBY}	V_{IN} = 24V, V_{EN} = 0V, I_{VCC} = 0, PGOOD = unconnected		0.35	0.55	mA
V_{CC} REGULATOR						
Output Voltage	V_{VCC}	6V ≤ V_{IN} ≤ 40V, I_{LOAD} = 6mA	5	5.25	5.5	V
V_{CC} Regulator Dropout		V_{IN} = 4.5V, I_{LOAD} = 25mA		0.18	0.45	V
V_{CC} Short-Circuit Output Current		V_{IN} = 5V	30	55	90	mA
V_{CC} Undervoltage Lockout	V_{CCUVLO}	V_{VCC} rising	3.8	4	4.2	V
V_{CC} Undervoltage Lockout Hysteresis				400		mV
ERROR AMPLIFIER (FB, COMP)						
FB Input-Voltage Set Point	V_{FB}		584	590	596	mV
FB Input Bias Current	I_{FB}	V_{FB} = 0.6V	-250		+250	nA
FB to COMP Transconductance	g_M	I_{COMP} = ±20µA	600	1200	1800	µS
Open-Loop Gain				80		dB
Unity-Gain Bandwidth		Capacitor from COMP to GND = 47pF		5		MHz

ELECTRICAL CHARACTERISTICS (continued)

(V_{IN} = 24V, V_{EN} = 5V, V_{GND} = V_{PGND} = 0V, C_{IN} = 1µF, C_{VCC} = 4.7µF, R_{RT} = 49.9kΩ, T_A = T_J = -40°C to +125°C, unless otherwise noted. Typical values are at T_A = +25°C.) (Note 2)

PARAMETER	SYMBOL	CONDITIONS	MIN	TYP	MAX	UNITS
$V_{COMP-RAMP}$ Minimum Voltage				200		mV
COMP Source/Sink Current	I_{COMP}	V_{COMP} = 1.4V	50	80	110	µA
ENABLE (EN)						
EN Input High	V_{EN_H}	V_{EN} rising	1.14	1.20	1.26	V
EN Input Low	V_{EN_L}	V_{EN} falling		1.05		V
EN Input Leakage Current	I_{EN}	V_{EN} = 5.5V	-1		+1	µA
OSCILLATOR						
Switching Frequency (100kHz)	f_{SW}	R_{RT} = 150kΩ	80	100	120	kHz
Switching Frequency (300kHz)	f_{SW}	R_{RT} = 49.9kΩ	270	300	330	kHz
Switching Frequency (1MHz)	f_{SW}	R_{RT} = 14.3kΩ	0.9	1	1.1	MHz
Switching Frequency Adjustment Range		(Note 3)	100		1000	kHz
RT Voltage	V_{RT}	R_{RT} = 49.9kΩ	1.15	1.2	1.25	V
PWM MODULATOR						
PWM Ramp Peak-to-Peak Amplitude	V_{RAMP}			1.5		V
PWM Ramp Valley	V_{VALLEY}			1.5		V
Minimum Controllable On-Time				70	125	ns
Maximum Duty Cycle		f_{SW} = 300kHz (R_{RT} = 49.9kΩ)	85	87.5		%
Minimum Low-Side On-Time		f_{SW} = 1MHz (R_{RT} = 49.9kΩ)		110		ns
OUTPUT DRIVERS/DRIVERS SUPPLY (V_{DRV})						
Undervoltage Lockout	V_{DRV_UVLO}	V_{DRV} rising	4.0	4.2	4.4	V
DRV Undervoltage Lockout Hysteresis				400		mV
DH On-Resistance		Low, sinking 100mA, V_{BST} - V_{LX} = 5V		1	3	Ω
		High, sourcing 100mA, V_{BST} - V_{LX} = 5V		1.5	4	
DL On-Resistance		Low, sinking 100mA, V_{DRV} = V_{CC} = 5.25V		1	3	
		High, sourcing 100mA, V_{DRV} = V_{CC} = 5.25V		1.5	4	
DH Peak Current		C_{LOAD} = 10nF, Sinking, V_{BST} - V_{LX} = 5V		3		A
		C_{LOAD} = 10nF, Sourcing, V_{BST} - V_{LX} = 5V		2		

40V, High-Performance Synchronous Buck Controller

ELECTRICAL CHARACTERISTICS (continued)

(V_{IN} = 24V, V_{EN} = 5V, V_{GND} = V_{PGND} = 0V, C_{IN} = 1µF, C_{VCC} = 4.7µF, R_{RT} = 49.9kΩ, T_A = T_J = -40°C to +125°C, unless otherwise noted. Typical values are at T_A = +25°C.) (Note 2)

PARAMETER	SYMBOL	CONDITIONS		MIN	TYP	MAX	UNITS
DL Peak Current		C_{LOAD} = 10nF	Sinking, V_{DRV} = V_{CC} = 5.25V		3		A
			Sourcing, V_{DRV} = V_{CC} = 5.25V		2		
DH, DL Break-Before-Make Time (Dead Time)					10		ns
SOFT-START							
Soft-Start Duration					2048		Switching Cycles
Reference Voltage Steps					64		Steps
CURRENT LIMIT/HICCUP							
Cycle-by-Cycle Valley Current-Limit Threshold Adjustment Range		V_{CSP} - V_{PGND}, valley limit = V_{LIM}/10	V_{LIM} = 0.3V		30		mV
			V_{LIM} = 3V		300		
LIM Reference Current	I_{LIM}	V_{LIM} = 0.3V to 3V, T_A = +25°C		45	50	55	µA
LIM Reference Current Temperature Coefficient					2300		ppm/°C
CSP Input Bias Current		V_{CSP} = 40V		-1		+1	µA
Number of Consecutive Current-Limit Events to Hiccup					7		Events
Hiccup Timeout					4096		Switching Cycles
Peak Low-Side Sink Current-Limit Threshold		V_{CSP} - V_{PGND}, sink limit = V_{LIM}/20, R_{ILIM} = 30kΩ, V_{LIM} = 1.5V, T_A = +25°C			75		mV
POWER-GOOD (PGOOD)							
PGOOD Threshold		V_{FB} rising		90	94	97.5	%V_{FB}
PGOOD Threshold Hysteresis		V_{FB} falling			2.65		%V_{FB}
PGOOD Output Low Voltage	V_{PGOOD_L}	I_{PGOOD} = 2mA, V_{EN} = 0V				0.4	V
PGOOD Output Leakage Current	I_{LEAK_PGOOD}	V_{PGOOD} = 40V, V_{EN} = 5V, V_{FB} = 1V		-1		+1	µA
THERMAL SHUTDOWN							
Thermal Shutdown Threshold		Temperature rising			+150		°C
Thermal Shutdown Hysteresis					20		°C

Note 2: All devices are 100% tested at room temperature and guaranteed by design over the specified temperature range.

Note 3: Select R_{RT} as: $R_{RT} = \frac{17.3 \times 10^9}{f_{SW} + (1 \times 10^{-7})(f_{SW}^2)}$, where f_{SW} is in Hertz.

40V, High-Performance, Synchronous Buck Controller

Pin Description

PIN	NAME	FUNCTION
1	IN	Regulator Input. Connect to the input rail of the buck converter. Bypass IN to PGND with a 100nF minimum ceramic capacitor. When operating in the 5V ±10% range, connect IN to V_{CC}.
2	V_{CC}	5.25V Linear Regulator Output. Bypass V_{CC} to PGND with a ceramic capacitor of at least 4.7µF when V_{CC} supplies MOSFET gate-driver current at DRV or 2.2µF when V_{CC} is not used to power DRV.
3	PGOOD	Open-Drain Power-Good Output. Pull up PGOOD to an external power supply or output with an external resistor.
4	EN	Active-High Enable Input. Pull EN to GND to disable the buck converter output. Connect to V_{CC} for always-on operation. EN can be used for power sequencing and as a UVLO adjustment input.
5	LIM	Current-Limit Input. Connect a resistor from LIM to GND to program the current-limit threshold from 30mV (R_{LIM} = 6kΩ) to 300mV (R_{LIM} = 60kΩ).
6	COMP	Error-Amplifier Output. Connect compensation network from COMP to FB or from COMP to GND.
7	FB	Feedback Input (Inverting Input of Error Amplifier). Connect FB to a resistive divider between the buck converter output and GND to adjust the output voltage from 0.6V up to 0.85 x IN.
8	RT	Oscillator-Timing Resistor Input. Connect a resistor from RT to GND to set the oscillator frequency from 100kHz to 1MHz.
9	GND	Analog Ground. Connect PGND and AGND together at a single point.
10	PGND	Power Ground. Use PGND as a return path for the low-side MOSFET gate driver.
11	DRV	Gate-Driver Supply Voltage. DRV is internally connected to the low-side driver supply. Bypass DRV to PGND with a 2.2µF minimum ceramic capacitor (see the *Typical Application Circuits*).
12	DL	Low-Side External MOSFET Gate-Driver Output. DL swings from DRV to PGND.
13	BST	Boost Flying Capacitor Connection. Internally connected to the high-side driver supply. Connect a ceramic capacitor of at least 100nF between BST and LX and a diode between BST and DRV for the high-side MOSFET gate-driver supply.
14	LX	Inductor Connection. Also serves as a return terminal for the high-side MOSFET driver current. Connect LX to the switching side of the inductor.
15	DH	High-Side External MOSFET Gate-Driver Output. DH swings from BST to LX.
16	CSP	Current-Sense Positive Input. Connect to the drain of low-side MOSFET with Kelvin connection.
—	EP	Exposed Pad. EP is internally connected to ground. Connect EP to a large copper ground plane to maximize thermal performance.

40V, High-Performance, Synchronous Buck Controller

Detailed Description

The MAX15046 synchronous step-down controller operates from a 4.5V to 40V input-voltage range and generates an adjustable output voltage from 85% of the input-voltage down to 0.6V while supporting loads up to 25A. As long as the device supply voltage is within 5.0V to 5.5V, the input power bus (V_{IN}) can be as low as 3.3V.

The MAX15046 offers adjustable switching frequency from 100kHz to 1MHz with an external resistor. The adjustable switching frequency provides design flexibility in selecting passive components. The MAX15046 adopts an adaptive synchronous rectification to eliminate external freewheeling Schottky diodes and improve efficiency. The device utilizes the on-resistance of the external low-side MOSFET as a current-sense element. The current-limit threshold voltage is resistor-adjustable from 30mV to 300mV and is temperature-compensated, so that the effects of the MOSFET $R_{DS(ON)}$ variation over temperature are reduced. This current-sensing scheme protects the external components from damage during output overloaded conditions or output short-circuit faults without requiring a current-sense resistor. Hiccup-mode current limit reduces power dissipation during short-circuit conditions. The MAX15046 includes a power-good output and an enable input with precise turn-on/-off threshold to be used for monitoring and for power sequencing.

The MAX15046 features internal digital soft-start that allows prebias startup without discharging the output. The digital soft-start function employs sink current limiting to prevent the regulator from sinking excessive current when the prebias voltage exceeds the programmed steady-state regulation level. The digital soft-start feature prevents the synchronous rectifier MOSFET and the body diode of the high-side MOSFET from experiencing dangerous levels of current while the regulator is sinking current from the output. The MAX15046 shuts down at a +150°C junction temperature to prevent damage to the device.

DC-DC PWM Controller

The MAX15046 step-down controller uses a PWM voltage-mode control scheme (see the *Functional Diagram*). Control-loop compensation is external for providing maximum flexibility in choosing the operating frequency and output LC filter components. An internal transconductance error amplifier produces an integrated error voltage at COMP that helps to provide higher DC accuracy. The voltage at COMP sets the duty cycle using a PWM comparator and a ramp generator. On the rising edge of an internal clock, the high-side n-channel MOSFET turns on and remains on until either the appropriate duty cycle or the maximum duty cycle is reached. During the on-time of the high-side MOSFET, the inductor current ramps up. During the second-half of the switching cycle, the high-side MOSFET turns off and the low-side n-channel MOSFET turns on. The inductor releases the stored energy as the inductor current ramps down, providing current to the output. Under overload conditions, when the inductor current exceeds the selected valley current-limit threshold (see the *Current-Limit Circuit (LIM)* section), the high-side MOSFET does not turn on at the subsequent clock rising edge and the low-side MOSFET remains on to let the inductor current ramp down.

Internal 5.25V Linear Regulator

An internal linear regulator (V_{CC}) provides a 5.25V nominal supply to power the internal functions and to drive the low-side MOSFET. Connect IN and V_{CC} together when using an external 5V ±10% power supply. The maximum regulator input voltage (V_{IN}) is 40V. Bypass IN to GND with a 1µF ceramic capacitor. Bypass the output of the linear regulator (V_{CC}) with a 4.7µF ceramic capacitor to GND. The V_{CC} dropout voltage is typically 180mV. When V_{IN} is higher than 5.5V, V_{VCC} is typically 5.25V. The MAX15046 also employs an undervoltage lockout circuit that disables the internal linear regulator when V_{VCC} falls below 3.6V (typical). The 400mV UVLO hysteresis prevents chattering on power-up/power-down.

MOSFET Gate Drivers (DH, DL)

DH and DL are optimized for driving large-size n-channel power MOSFETs. Under normal operating conditions and after startup, the DL low-side drive waveform is always the complement of the DH high-side drive waveform, with controlled dead time to prevent crossconduction or "shoot-through." An adaptive dead-time circuit monitors the DH and DL outputs and prevents the opposite-side MOSFET from turning on until the MOSFET is fully off. Thus, the circuit allows the high-side driver to turn on only when the DL gate driver has turned off preventing the low side (DL) from turning on until the DH gate driver has turned off.

The adaptive driver dead time allows operation without shoot-through with a wide range of MOSFETs, minimizing delays and maintaining efficiency. There must be a low-resistance, low-inductance path from DL and DH to the MOSFET gates for the adaptive dead-time circuits

MAX15046 stops both DL and DH drivers and waits for 4096 switching cycles (hiccup timeout delay) before attempting a new soft-start sequence. The hiccup-mode protection remains active during the soft-start time.

Undervoltage Lockout

The MAX15046 provides an internal undervoltage lockout (UVLO) circuit to monitor the voltage on V_{CC}. The UVLO circuit prevents the MAX15046 from operating when V_{CC} is lower than V_{UVLO}. The UVLO threshold is 4V, with 400mV hysteresis to prevent chattering on the rising/falling edge of the supply voltage. DL and DH stay low to inhibit switching when the device is in undervoltage lockout.

Thermal-Overload Protection

Thermal-overload protection limits total power dissipation in the MAX15046. When the junction temperature of the device exceeds +150°C, an on-chip thermal sensor shuts down the device, forcing DL and DH low, which allows the device to cool. The thermal sensor turns the device on again after the junction temperature cools by 20°C. The regulator shuts down and soft-start resets during thermal shutdown. Power dissipation in the LDO regulator and excessive driving losses at DH/DL trigger thermal-overload protection. Carefully evaluate the total power dissipation (see the *Power Dissipation* section) to avoid unwanted triggering of the thermal-overload protection in normal operation.

Applications Information

Effective Input-Voltage Range

The MAX15046 operates from 4.5V to 40V input supplies and regulates output down to 0.6V. The minimum voltage conversion ratio (V_{OUT}/V_{IN}) is limited by the minimum controllable on-time. For proper fixed-frequency PWM operation, the voltage conversion ratio must obey the following condition:

$$\frac{V_{OUT}}{V_{IN}} > t_{ON(MIN)} \times f_{SW}$$

where $t_{ON(MIN)}$ is 125ns and f_{SW} is the switching frequency in Hertz. Pulse skipping occurs to decrease the effective duty cycle when the desired voltage conversion does not meet the above condition. Decrease the switching frequency or lower the input voltage V_{IN} to avoid pulse skipping.

The maximum voltage conversion ratio is limited by the maximum duty cycle (D_{max}):

$$\frac{V_{OUT}}{V_{IN}} < D_{max} - \frac{D_{max} \times V_{DROP2} + (1-D_{max}) \times V_{DROP1}}{V_{IN}}$$

where V_{DROP1} is the sum of the parasitic voltage drops in the inductor discharge path, including synchronous rectifier, inductor, and PCB resistance. V_{DROP2} is the sum of the resistance in the charging path, including high-side switch, inductor, and PCB resistance. In practice, provide adequate margin to the above conditions for good load-transient response.

Setting the Output Voltage

Set the MAX15046 output voltage by connecting a resistive divider from the output to FB to GND (Figure 2). Select R_2 from between 4kΩ and 16kΩ. Calculate R_1 with the following equation:

$$R_1 = R_2 \left[\left(\frac{V_{OUT}}{V_{FB}} \right) - 1 \right]$$

where V_{FB} = 0.59V (see the *Electrical Characteristics* table) and V_{OUT} can range from 0.6V to (0.85 x V_{IN}).

Resistor R_1 also plays a role in the design of the Type III compensation network. Review the values of R_1 and R_2 when using a Type III compensation network (see the *Type III Compensation Network (Figure 4)* section).

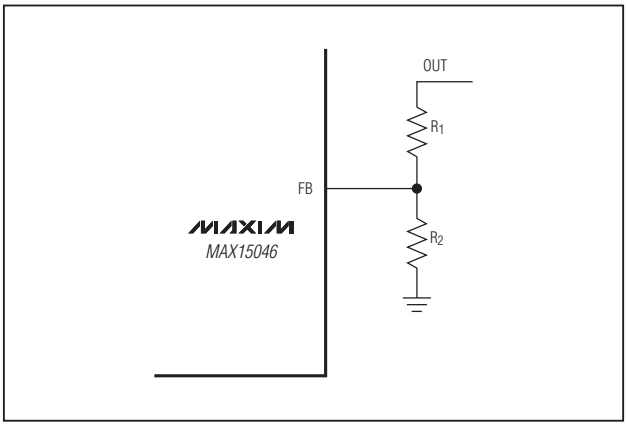

Figure 2. Adjustable Output Voltage

40V, High-Performance, Synchronous Buck Controller

Setting the Switching Frequency

An external resistor connecting RT to GND sets the switching frequency (f_{SW}). The relationship between f_{SW} and R_{RT} is:

$$R_{RT} = \frac{17.3 \times 10^9}{f_{SW} + (1 \times 10^{-7}) \times (f_{SW}^2)}$$

where f_{SW} is in kHz and R_{RT} is in kΩ. For example, a 300kHz switching frequency is set with R_{RT} = 49.9kΩ. Higher frequencies allow designs with lower inductor values and less output capacitance. Peak currents and I^2R losses are lower at higher switching frequencies, but core losses, gate-charge currents, and switching losses increase.

Inductor Selection

Three key inductor parameters must be specified for operation with the MAX15046: inductance value (L), inductor saturation current (I_{SAT}), and DC resistance (R_{DC}). To determine the inductance, select the ratio of inductor peak-to-peak AC current to DC average current (LIR) first. For LIR values that are too high, the RMS currents are high, and therefore I^2R losses are high. Use high-valued inductors to achieve low LIR values. Typically, inductor resistance is proportional to inductance for a given package type, which again makes I^2R losses high for very low LIR values. A good compromise between size and loss is a 30% peak-to-peak ripple current to average-current ratio (LIR = 0.3). The switching frequency, input voltage, output voltage, and selected LIR determine the inductor value as follows:

$$L = \frac{V_{OUT}(V_{IN} - V_{OUT})}{V_{IN} \times f_{SW} \times I_{OUT} \times LIR}$$

where V_{IN}, V_{OUT}, and I_{OUT} are typical values. The switching frequency is set by R_T (see *Setting the Switching Frequency* section). The exact inductor value is not critical and can be adjusted to make trade-offs among size, cost, and efficiency. Lower inductor values minimize size and cost, but also improve transient response and reduce efficiency due to higher peak currents. On the other hand, higher inductance increases efficiency by reducing the RMS current.

Find a low-loss inductor with the lowest possible DC resistance that fits in the allotted dimensions. The saturation current rating (I_{SAT}) must be high enough to ensure that saturation cannot occur below the maximum current-limit value ($I_{CL(MAX)}$), given the tolerance of the on-resistance of the low-side MOSFET and of the LIM reference current (I_{LIM}). Combining these conditions, select an inductor with a saturation current (I_{SAT}) of:

$$I_{SAT} \geq 1.35 \times I_{CL(TYP)}$$

where $I_{CL(TYP)}$ is the typical current-limit set point. The factor 1.35 includes $R_{DS(ON)}$ variation of 25% and 10% for the LIM reference current error. A variety of inductors from different manufacturers are available to meet this requirement (for example, Vishay IHLP-4040DZ-1-5 and other inductors from the same series).

Setting the Valley Current Limit

The minimum current-limit threshold must be high enough to support the maximum expected load current with the worst-case low-side MOSFET on-resistance value as the $R_{DS(ON)}$ of the low-side MOSFET is used as the current-sense element. The inductor's valley current occurs at $I_{LOAD(MAX)}$ minus one half of the ripple current. The minimum value of the current-limit threshold voltage (V_{ITH}) must be higher than the voltage on the low-side MOSFET during the ripple-current valley,

$$V_{ITH} > R_{DS(ON,MAX)} \times I_{LOAD(MAX)} \times \left(1 - \frac{LIR}{2}\right)$$

where $R_{DS(ON,MAX)}$ in Ω is the maximum on-resistance of the low-side MOSFET at maximum load current $I_{LOAD(MAX)}$ and is calculated from the following equation:

$$R_{DS(ON,MAX)} = R_{DS(ON)} \times [1 + TC_{MOSFET} \times (T_{MAX} - T_{AMB})]$$

where $R_{DS(ON)}$ (in Ω is the on-resistance of the low-side MOSFET at ambient temperature T_{AMB} (in degrees Celsius), TC_{MOSFET} is the temperature coefficient of the low-side MOSFET in ppm/°C, and T_{MAX} (in degrees Celsius) is the temperature at maximum load current $I_{LOAD(MAX)}$. Obtain the $R_{DS(ON)}$ and TC_{MOSFET} from the MOSFET data sheet.

Connect an external resistor (R_{LIM}) from LIM to GND to adjust the current-limit threshold, which is temperature-compensated with a temperature coefficient of -2300ppm/°C. The relationship between the current-limit threshold (V_{ITH}) and R_{LIM} is:

$$R_{LIM} = \frac{10 \times V_{ITH}}{50 \times 10^{-6} \times \left[1 + 2300 \times (T_{MAX} - T_{AMB})\right]}$$

where R_{LIM} is in Ω, V_{ITH} is in V, T_{MAX} and T_{AMB} are in °C.

An R_{LIM} resistance range of 6kΩ to 60kΩ corresponds to a current-limit threshold of 30mV to 300mV. Use 1% tolerance resistors when adjusting the current limit to minimize error in the current-limit threshold.

Input Capacitor

The input filter capacitor reduces peak current drawn from the power source and reduces noise and voltage ripple on the input caused by the switching circuitry. The input capacitor must meet the ripple current requirement (I_{RMS}) imposed by the switching currents as defined by the following equation:

$$I_{RMS} = I_{LOAD(MAX)} \frac{\sqrt{V_{OUT}(V_{IN} - V_{OUT})}}{V_{IN}}$$

I_{RMS} attains a maximum value when the input voltage equals twice the output voltage ($V_{IN} = 2V_{OUT}$), so $I_{RMS(MAX)} = I_{LOAD(MAX)}/2$. For most applications, nontantalum capacitors (ceramic, aluminum, polymer, or OS-CON) are preferred at the inputs due to the robustness of nontantalum capacitors to accommodate high inrush currents of systems being powered from very low impedance sources. Additionally, two (or more) smaller-value low-ESR capacitors should be connected in parallel to reduce high-frequency noise.

Output Capacitor

The key selection parameters for the output capacitor are capacitance value, ESR, and voltage rating. These parameters affect the overall stability, output ripple voltage, and transient response. The output ripple has two components: variations in the charge stored in the output capacitor, and the voltage drop across the capacitor's ESR caused by the current flowing into and out of the capacitor:

$$\Delta V_{RIPPLE} = \Delta V_{ESR} + \Delta V_Q$$

The output-voltage ripple as a consequence of the ESR and the output capacitance is:

$$\Delta V_{ESR} = I_{P-P} \times ESR$$

$$\Delta V_Q = \frac{I_{P-P}}{8 \times C_{OUT} \times f_{SW}}$$

$$I_{P-P} = \left(\frac{V_{IN} - V_{OUT}}{f_{SW} \times L}\right) \times \left(\frac{V_{OUT}}{V_{IN}}\right)$$

where I_{P-P} is the peak-to-peak inductor current ripple (see the *Inductor Selection* section). Use these equations for initial capacitor selection. Decide on the final values by testing a prototype or an evaluation circuit.

Check the output capacitor against load-transient response requirements. The allowable deviation of the output voltage during fast load transients determines the capacitor output capacitance, ESR, and equivalent series inductance (ESL). The output capacitor supplies the load current during a load step until the controller responds with a higher duty cycle. The response time ($t_{RESPONSE}$) depends on the closed-loop bandwidth of the converter (see the *Compensation Design* section). The resistive drop across the ESR of the output capacitor, the voltage drop across the ESL (ΔV_{ESL}) of the capacitor, and the capacitor discharge, cause a voltage droop during the load step.

Use a combination of low-ESR tantalum/aluminum electrolytic and ceramic capacitors for improved transient load and voltage ripple performance. Nonleaded capacitors and capacitors in parallel help reduce the ESL. Keep the maximum output-voltage deviation below the tolerable limits of the load. Use the following equations to calculate the required ESR, ESL, and capacitance value during a load step:

$$ESR = \frac{\Delta V_{ESR}}{I_{STEP}}$$

$$C_{OUT} = \frac{I_{STEP} \times t_{RESPONSE}}{\Delta V_Q}$$

$$ESL = \frac{\Delta V_{ESL} \times t_{STEP}}{I_{STEP}}$$

$$t_{RESPONSE} \cong \frac{1}{3 \times f_O}$$

where I_{STEP} is the load step, t_{STEP} is the rise time of the load step, $t_{RESPONSE}$ is the response time of the controller, and f_O is the closed-loop crossover frequency.

Appendix B

PIC18F4550 Microprocessor

Appendix C

TLE5205-2 Motor Controller

1 Overview

1.1 Features

- Delivers up to 5 A continuous 6 A peak current
- Optimized for DC motor management applications
- Operates at supply voltages up to 40 V
- Very low $R_{DS\ ON}$; typ. 200 mΩ @ 25 °C per switch
- Output full short circuit protected
- Overtemperature protection with hysteresis and diagnosis
- Short circuit and open load diagnosis with open drain error flag
- Undervoltage lockout
- CMOS/TTL compatible inputs with hysteresis
- No crossover current
- Internal freewheeling diodes
- Wide temperature range; – 40 °C < T_j < 150 °C

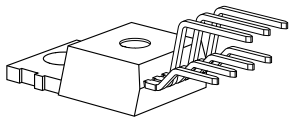

P-TO220-7-11

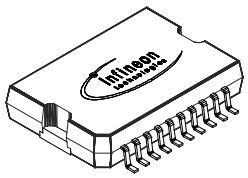

P-DSO-20-12

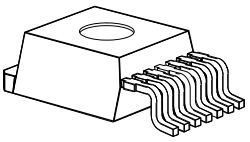

P-TO263-7-1

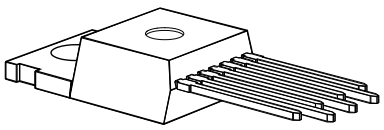

P-TO220-7-12

Type	Ordering Code	Package
TLE 5205-2	Q67000-A9283	P-TO220-7-11
TLE 5205-2GP	Q67006-A9237	P-DSO-20-12
TLE 5205-2G	Q67006-A9325	P-TO263-7-1
TLE 5205-2S	Q67000-A9324	P-TO220-7-12

Description

The TLE 5205-2 is an integrated power H-bridge with DMOS output stages for driving DC-Motors. The part is built using the Infineon multi-technology process SPT® which allows bipolar and CMOS control circuitry plus DMOS power devices to exist on the same monolithic structure.

Operation modes forward (cw), reverse (ccw), brake and high impedance are invoked from just two control pins with TTL/CMOS compatible levels. The combination of an extremely low $R_{DS\ ON}$ and the use of a power IC package with low thermal resistance and high thermal capacity helps to minimize system power dissipation. A blocking capacitor at the supply voltage is the only external circuitry due to the integrated freewheeling diodes.

1.2 Pin Configuration (top view)

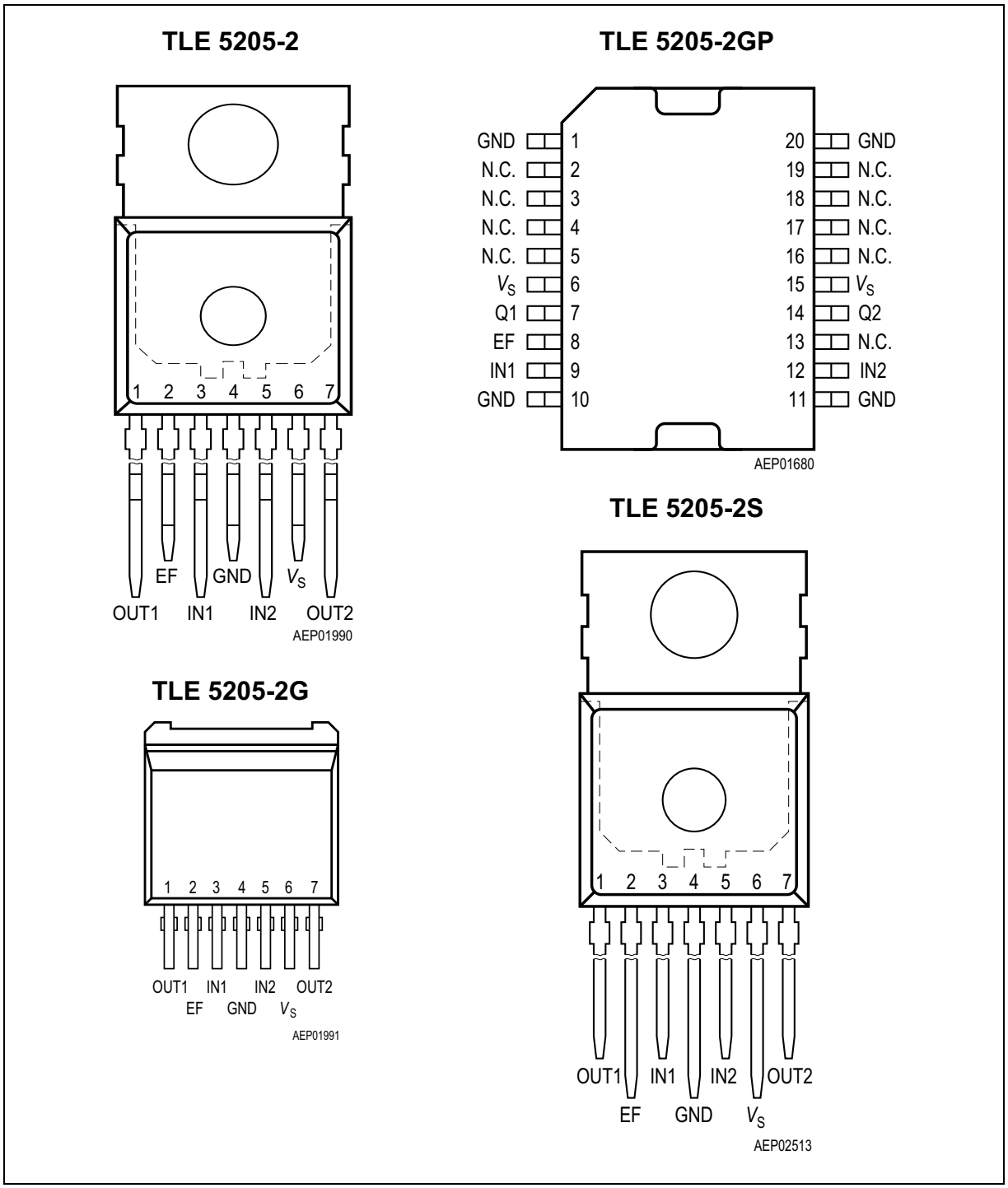

Figure 1

1.3 Pin Definitions and Functions

Pin No. P-TO220	Pin No. P-DSO	Symbol	Function
1	7	OUT1	**Output of Channel 1;** Short-circuit protected; integrated freewheeling diodes for inductive loads.
2	8	EF	**Error Flag;** TTL/CMOS compatible output for error detection; (open drain)
3	9	IN1	**Control Input 1;** TTL/CMOS compatible
4	1, 10, 11, 20	GND	**Ground;** internally connected to tab
5	12	IN2	**Control Input 2;** TTL/CMOS compatible
6	6, 15	V_S	**Supply Voltage;** block to GND
7	14	OUT2	**Output of Channel 2;** Short-circuit protected; integrated freewheeling diodes for inductive loads.
–	2, 3, 4, 5, 16, 17, 18, 19	N.C.	**Not Connected**

1.4 Functional Block Diagram

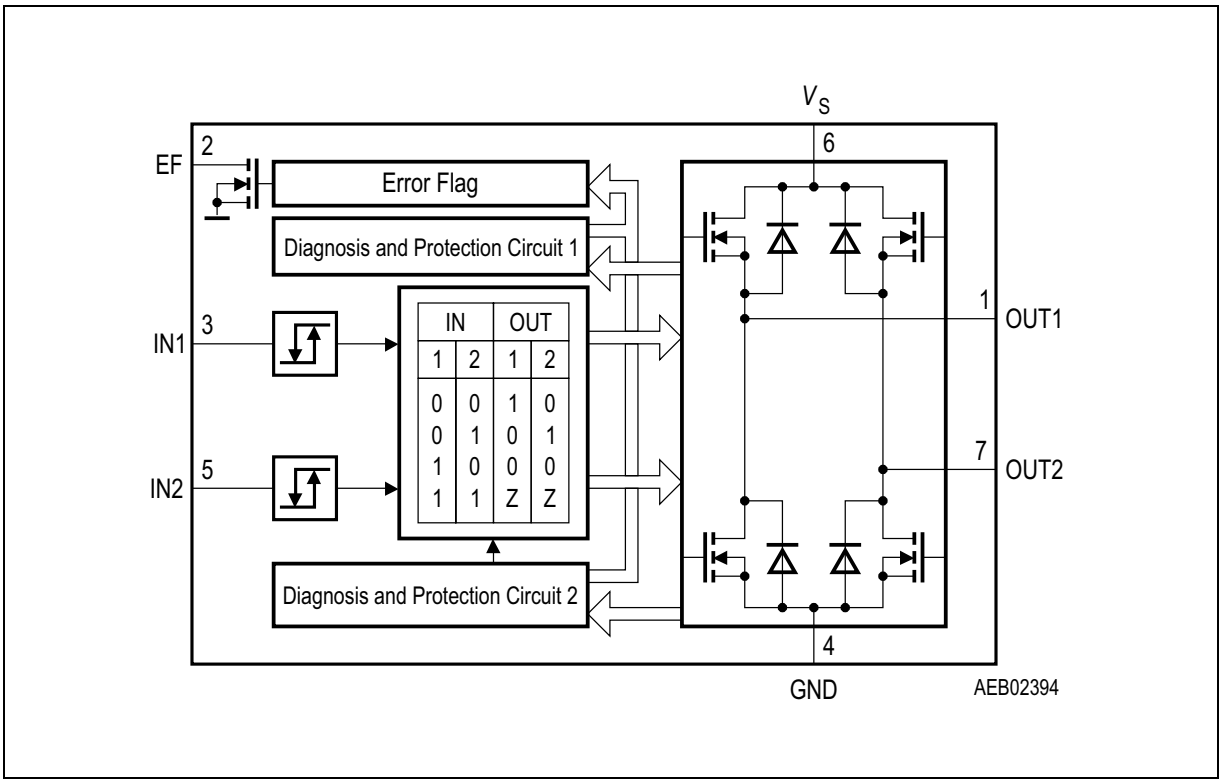

Figure 2 Block Diagram

1.5 Circuit Description

Input Circuit

The control inputs consist of TTL/CMOS-compatible schmitt-triggers with hysteresis. Buffer amplifiers are driven by this stages.

Output Stages

The output stages consist of a DMOS H-bridge. Integrated circuits protect the outputs against short-circuit to ground and to the supply voltage. Positive and negative voltage spikes, which occur when switching inductive loads, are limited by integrated freewheeling diodes.
A monitoring circuit for each output transistor detects whether the particular transitor is active and in this case prevents the corresponding source transistor (sink transistor) from conducting in sink operation (source operation). Therefore no crossover currents can occur.

1.6 Input Logic Truth Table

Functional Truth Table

IN1	IN2	OUT1	OUT2	Comments
L	L	H	L	Motor turns clockwise
L	H	L	H	Motor turns counterclockwise
H	L	L	L	Brake; both low side transistors turned-ON
H	H	Z	Z	Open circuit detection

Notes for Output Stage

Symbol	Value
L	Low side transistor is turned-ON High side transistor is turned-OFF
H	High side transistor is turned-ON Low side transistor is turned-OFF
Z	High side transistor is turned-OFF Low side transistor is turned-OFF